



**FINAL REPORT**

**Understanding of the degree to which parameters affect the  
subsurface natural gas migration with significant flow rates**

Prepared for the Pipeline and Hazardous Material Safety Administration (PHMSA)

Grant Number: 693JK32010011POTA

Grant Title: “Validating Models for Predicting Gas Migration and Mitigating its Occurrence/  
Consequence”

Reporting Period: December 2020 – December 2023

**April 29, 2024**

Prepared In Partnership with Colorado State University and Southern Methodist University

**J. R. R. Navodi Jayarathne<sup>1</sup>, Kathleen M. Smits<sup>1,2</sup>, Stuart N. Riddick<sup>2</sup>, Daniel Zimmerle<sup>2</sup>**

<sup>1</sup> Department of Civil and Environmental Engineering, Southern Methodist University, Dallas, Texas 75205, USA

<sup>2</sup> Energy Institute, Colorado State University, Fort Collins, Colorado 80524, USA

## **Legal Notice**

This research was funded in part under the Department of Transportation (DOT) Pipeline and Hazardous Materials Safety Administration (PHMSA) Pipeline Safety Research and Development Program (Project#: 693JK32010011POTA). The views and conclusions contained in this document are those of the authors and should not be interpreted as representing the official policies, either expressed or implied, of the Pipeline and Hazardous Materials Safety Administration or the U.S. Government.

## **Acknowledgments**

The project team would like to thank PHMSA for providing funding to perform this research. The research would not have been possible without the help of industry partners including Southern California Gas Company, Consolidated Edison, Xcel Energy, Pacific Gas and Electric, and Phillips 66, among others. In addition, special thanks to industry partners who provided essential site access and data.

## **Executive Summary**

This report represents the final report for project 693JK32010011POTA “Validating Models for Predicting Gas Migration and Mitigating its Occurrences/Consequences.”

The primary objectives of the project were 1) to develop methods and characterize belowground transient behavior of natural gas (NG) leaked from belowground transportation pipelines, and 2) link the understanding to operator and first responder practices through recommendations that could be applied in the field. To accomplish the project’s objective, eight tasks were outlined with specific deliverables and activities. The work was conducted with a combined team of researchers from Colorado State University, Fort Collins, CO, and Southern Methodist University, Dallas, TX. In conjunction with this academic cooperation, an industry-state coalition was established with 12 partners across both sectors. The partners actively engaged with researchers through industry-advisory meetings, experimental collaborations, and result reviews, conducted both online and in-person. This concerted effort ensured data and information were collected and communicated through appropriate avenues. The collaborative efforts of all partners resulted in a more comprehensive understanding of transient NG transport behavior, directly informing response protocols for operators and first responders.

Controlled, field-scale experiments consisted of testing the effects of diverse leakage scenarios, with a special focus on underground natural gas (NG) leaks with moderate to high flow rates (>100 scfh) that can produce explosive concentrations within the subsurface and in nearby substructures. In total, 150 experiments were conducted at the custom-built Methane Emissions Technology Evaluation Center (METEC) belowground pipeline testbeds, designed to simulate both urban/suburban and rural environments. During the experiments, data were collected to analyze the comprehensive transient behavior of NG during and after belowground pipeline leakage events. This encompasses the unsteady state, characterized by the period from the onset of the leak until it achieves a quasi-steady state; the quasi-steady state where the inflow of gas from the leak equilibrates with the outflow to the atmosphere; as well as the subsequent unsteady state following the termination of gas flow from the leak. In this context, the term "unsteady state" refers to the spatial fluctuation of methane over time, resulting in either the lateral expansion of the plume away from the leak point or its contraction post-termination of the leak. Contrastingly, the "quasi-steady state" denotes a stabilized leak condition where lateral expansion ceases while maintaining the emission of gas from the soil to the atmosphere. METEC experimental results

were used to understand the belowground distribution of the NG plume, gas migration extent and rate, as well as critical parameter combinations that can influence gas migration rates and extents.

Numerical model simulations expanded upon the experimental results to consider other environmental and operating conditions not tested in the field: additional soil types, surface conditions, and belowground infrastructure complexities. Simulated results generated rates and extents of NG transport under different environmental and operating conditions. Based on the numerical findings, a second round of field-scale experiments was conducted focused on the soil-to-atmospheric transport of gas, with findings later incorporated into additional numerical simulations.

The project outputs included 12 peer-reviewed publications (8 published and 4 in review), 23 conference presentations and posters, 2 invited presentations, 3 METEC Research Alerts, and reference materials for first responders to include, as appropriate, in training materials. References and links to the various outputs can be found under Deliverable 17 of this report.

## **Key findings**

- The site conditions which increase the speed and extent of belowground gas transport from leaking pipelines include (in priority order): 1) subsurface soil fractures or open utilities (e.g. an empty conduit), 2) surface covers (snow, rain, and pavement), and 3) disturbed soil conditions (e.g. trenched/backfilled soil). In comparison, 4) soil type and pipeline depths between 3 ft and 6 ft have little influence on speed and extent. Finally, 5) soil moisture has a negative impact (i.e., an increase in soil moisture saturation decreases the lateral migration of leaked gas). Combinations of conditions can increase the influence on both the rate and extent of gas transport.
- Changes in surface conditions impact how far and how fast the gas travels below the ground. Moisture, snow, and asphalt can block gas from escaping the surface and result in gas moving both downwards and outwards away from the leak location. For the conditions tested, in the presence of asphalt, snow, or rain (wet surface), gas can spread up to 3-4 times further and 3.5 times faster than the equivalent leak scenario under dry soil conditions.
- The presence of a subsurface soil fracture or open conduit enhances belowground gas movement. For the scenarios tested, gas that can partially enter an adjacent fracture or

conduit can migrate ~ 4 and 5 times farther over 24 hours and 2-months, respectively, compared to a no-fracture/conduit condition.

- The methane surface expression is not representative of the size of the belowground leak. For example, under wet soil conditions, negligible methane concentrations are found at the surface while the largest accumulation of gas is found at shallow depths below ground surface (BGS).
- An increase in leak rate does not proportionally increase the gas migration rate and distance. High leak rates result in faster, and initially further, gas migrations for the high concentration contours close to the leak location but high leak rates have little influence on the low concentration contours farther from the leak location compared to lower leak rates.
- Over time when steady or a quasi-steady state is achieved, smaller and larger leak rates may result in similar areas of influence. Although the concentrations will vary with distance, the area of influence is often similar. This implies that, for established unresolved leaks that have persisted over time, the locations commonly considered unsafe for high leak rate scenarios should also be considered for unresolved low leak rate scenarios.
- Leak termination does not immediately remove high belowground concentrations, especially in the presence of snow, moisture, or asphalt conditions. For the conditions tested, gas remained in the soil at concentrations above 10% LEL for up to 14 days. Therefore, effort should be made to vent the soil after the leak was terminated, especially in the presence of snow, moisture, and asphalt.
- Because gas remains within the soil due to reduced venting in snow, moisture, and/or asphalt conditions, gas can continue to migrate away from the leak source via diffusion after leak termination. This is particularly critical for Grade 1 (hazardous) leaks, which are, by definition, near buildings.
- While natural gas is composed mostly of methane, the ratio of other gases (e.g. ethane, propane) affects the gas behavior as it moves underground. As the gas density increases, the potential for gas build-up underground increases and lateral migration increases. For the gas compositions tested, higher ethane and propane composition increase migration distance by 3 times and retention duration by 6 times.
- Atmospheric methane concentrations do not always give a clear indication of how large a leak could be; the severity of a leak may be underestimated due to variations in

atmospheric, surface, or subsurface conditions. Therefore, evidence from this study suggests that the criteria for the establishment of a hot zone should be expanded. A hot zone should be considered even if the threshold of 20% LEL has not been exceeded when any of the following is observed at the leak site:

- Waterlogged soil
  - Snow cover
  - Ice on the surface
  - Asphalt on surface
  - High winds
  - Very sunny conditions
  - Nighttime
- The hot zone radius should be increased from the existing 150-ft radius to a 300-ft radius for any leak where the threshold limit value of 20% LEL is observed in open spaces.

### **Further potential research:**

Based on the findings presented in this project, we propose several areas for further research.

- While this study tested many conditions, other factors should be considered for future experimental and numerical studies, including the effect of soil terrain and varying atmospheric conditions.
- There is a need for a risk-based assessment method to estimate how far and fast gas has potentially moved underground during a leak incident, and what conditions increase or decrease the likelihood of gas movement. Additional work should focus on methods to minimize risk by rapidly assessing operating conditions at the incident location. Through our current work, we have identified scenarios impacting the speed and extent of gas movement; however, there are currently no guidelines that prioritize combinations of diverse conditions and articulate how this prioritization can be linked with operator practice.
- There are no settled methods for effective leak quantification for flow and gathering lines, or for effective leak detection on gathering lines. Alternative methods are needed to quickly and efficiently detect leaks and quantify emissions using readily available

instrumentation linked and field-deployable algorithms. Simple and rapid methods would enable better prioritization of underground NG leak response efforts to mitigate both risk and greenhouse gas emissions. Experiments in this and our prior projects identified methods to quantify emission rates using limited knowledge of the subsurface and/or limited gas concentration measurements above ground, using only existing operator leak detection equipment. However, these methods need additional development and testing before field application.

While soil aeration systems are simple and oftentimes considered standard practice, the design, operation, and monitoring of soil aeration systems remains understudied. Many chemical and physical processes occur belowground that control the performance of aeration operations to include the chemical composition of the gas, air/gas flow rates through the soil and the flow path of the air relative to the gas location. However, such factors are generally not considered in aeration system design and gas mitigation operations. Additional research is needed to guide the design, operation, and monitoring of natural gas soil aeration systems that incorporate site specific, yet easily attainable, information.

# **Table of Contents**

Executive Summary .....	3
Key findings.....	4
Further potential research .....	6
Table of Contents .....	8
Table of Figures .....	12
List of Tables .....	15
List of Acronyms .....	16
1. Introduction.....	17
1.1 Background and Objectives .....	17
1.2 Scope of Work .....	19
Task 1: Establish a collaborative study structure.....	19
Task 2: Survey existing first responder operational practices .....	19
Task 3: Methods Development .....	20
Task 3.1: Sensor Testing.....	20
Task 3.2: Installation of Test Sensors at METEC.....	20
2. Deliverable 2: Survey existing first responder operational practices.....	22
2.1 Objectives .....	22
2.2 Activities.....	22
2.3 Observations .....	22
2.4 Key findings.....	24
3. Deliverable 3: Methods for estimating gas migration and leak size from readily obtained measurements at a leak event.....	26
3.1 Objectives .....	26



3.2 Activities .....	26
3.3 Experimental Method.....	26
3.4 Numerical Method .....	28
3.5 Selection of a Baseline Scenario .....	30
3.6 Comparison Matrices .....	30
4. Deliverable 4, 5: Testbed completion and measurement points installment.....	32
4.1 Objectives .....	32
4.2 Activities .....	32
4.3 Rural Testbed.....	32
4.4 Urban Testbed.....	33
4.5 Controlled Releases .....	36
5. Deliverable 6: Approaches to the design, operation, and monitoring of natural gas soil venting systems.....	37
5.1 Objectives .....	37
5.2 Current state of practice.....	37
5.3 Selected soil venting model .....	38
5.4 Preliminary simulations .....	38
6. Deliverables 7, 8, 9, 12, and 14: Comprehensive data sets and understanding of the degree to which parameters affect the subsurface natural gas migration with significant flow rates .....	43
6.1 Objective.....	43
6.2 Activities .....	43
6.3 Summary of Experiments Conducted .....	44
6.4 Effect of Leak Rate .....	46
6.5 Effect of Surface Condition .....	48
6.6 Effect of Gas Composition.....	51
6.7 Effect of Combined Surface Subsurface Anomalies .....	53

6.8 Belowground Flammable Threat zone and Methane Contaminated Zone .....	54
6.9 Surface Expression of Belowground NG Plumes .....	56
6.10 Key Findings .....	58
7. Deliverable 13: Modeling tool to predict the behavior of underground leaks with significant flow rates .....	61
7.1 Objective: .....	61
7.2 Development and Optimization of Simulation Domain .....	61
7.3 Variation in subsurface CH <sub>4</sub> migration extent and rate .....	62
7.4 Long-term Behavior Subsurface of NG Leaks .....	68
7.5 Key Findings .....	70
8. Deliverable 15: Underground natural gas pipeline leak: recommendations for first responders .....	72
8.1 Objective: .....	72
8.2 Key Findings .....	72
9. Deliverable 17: Project Outputs .....	74
9.1 Objective: .....	74
9.2 Peer Reviewed Publications/ Proceedings .....	74
9.3 Conference Presentation and Posters .....	81
9.4 Invited Presentations .....	84
9.5 METEC Research Alerts .....	85
9.6 Media Reports .....	85
10. References .....	86
11. Appendix .....	89

## Appendices

- Appendix 1: Survey of first responder operational practices: First responder operational practices when attended large pipeline leak events
- Appendix 2: Performance Testing of SGX Integrated Infrared (INIR) sensor in subsurface methane detection
- Appendix 3: RPLUME / UPSIDE Data Management Protocol
- Appendix 4: Report on a Practical Approach to the Design, Operation, and Monitoring of Soil Aeration
- Appendix 5: Understanding of the degree to which parameters affect the subsurface natural gas migration with significant flow rates: Experimental Report
- Appendix 6: Understanding of the degree to which parameters affect the subsurface natural gas migration with significant flow rates: Simulation Report
- Appendix 7: Underground Natural Gas Pipeline Leak Behavior: Connecting gas migration understanding to first responder protocols

## **Table of Figures**

- Figure 1: An idealized schematic of gas leakage from an underground pipeline and the complex mechanisms that affect the gas migration and intrusion into a basement or substructure. Arrows represent gas flow velocity and contour the methane percent of the lower explosive limit. Arrow lengths are proportional to the logarithm of the velocity magnitude. Modelling by PIs. .... 18
- Figure 2: Schematic of the rural testbed profile with locations for belowground Emission points and sensor locations for methane (INIR-type) and soil moisture/temperature/matric potential sensors. Specific distances from the emission point and depths from the surface are also shown. .... 33
- Figure 3 Schematic of the testbed profile for the structure with a basement. (a) Plan view of the testbed with the basement structure (b) East-West profile with a grass cover and (c) North-South profile with an asphalt pavement. Location of gas release points, sensor locations, the utility pipelines, and the location for each type of sensors are also shown. .... 34
- Figure 4: Construction of (a) slab-on-grade and (b) basement foundations for structures, PVC sleeves for CH<sub>4</sub> concentration sensors, and the trench running from the structures towards the road are also visible. (c) ground view and (d) aerial view of the completed Urban testbed with three structures, and the asphalt pavement in front of the middle structure. .... 35
- Figure 5: The change in the residual CH<sub>4</sub> concentration at the bottom of the venting bar hole during one hour of soil venting under venting pressures of (a) 0 atm, (c) 0.2 atm, and (e) 0.5 atm, respectively. The surface pressure in the model was given as the gauge pressure of 0 atm. .... 39
- Figure 6: The radius of influences in six soil conditions with the venting pressure from 0 atm to 0.5 atm in the scenarios with a venting bar and three venting bar holes. .... 40
- Figure 7: The variation of venting flow rates in six soil permeability scenarios based on one venting bar hole (1 BH) and three venting barhole (3BH) scenarios. The red and blue lines present the venting flow rate with the venting pressure of 0.2 atm and 0.5 atm, respectively. The solid line indicates the scenario with a venting bar hole (1 BH). The dashed line describes the scenario with three venting bar holes (3 BH) .... 41
- Figure 8: Subsurface methane concentration distribution at 6 hours after leak initiation and 24 hours after leak termination experiments with leak rates 10, 35, 50, 100, and 200 slpm. (a), (c), (e), (g), (i) are vertical profiles for 6 hours after leak initiation, and (b), (d), (f), (h), (j) are vertical profiles 24 hours after leak termination. The respective belowground profile key for each experiment, the location of the leak point, and measurement points are also shown. Surface and subsurface measurement points are shown in black and white dots

respectively. Profiles are created considering a homogeneous soil structure along all directions.....	47
Figure 9: Subsurface methane concentration distribution at 6 and 24 hours after leak initiation and 24 hours after leak termination for Grass-Dry, Asphalt-Dry, Grass-Moist, and Grass-Snow experiments. (a), (d), (g), (j), and (b), (e), (h), (k) are vertical profiles for 6 and 24 hours respectively after leak initiation. (c), (f), (i), (l) are vertical profiles for 24 hours after leak termination. The respective belowground profile key for each experiment, the location of the leak point, measurement points, and the asphalt layer are also shown. Surface and subsurface measurement points are shown in black and white dots respectively. Profiles are created considering a homogeneous soil structure along all directions.....	49
Figure 10: Variation in migration rate for 0.01%, 0.5%, 5%, and 15% CH <sub>4</sub> (v/v) contours under (a) Grass-Dry, (b) Asphalt-Dry, (c) Grass-Moist, (d) Grass-Snow surface conditions. The distances between each measurement point are represented by dotted vertical lines at 1.2, 3.2, and 4.6 m along the x-axis.....	51
Figure 11: Variation in flammable limits (10%LEL=0.5% CH <sub>4</sub> (v/v), LEL = 5% CH <sub>4</sub> (v/v), and UEL=15% CH <sub>4</sub> (v/v)) (a) duration and (b) travel distance for 20 scfh (10 slpm) leaks under different gas compositions of methane, ethane, propane, and air.....	52
Figure 12: Subsurface methane concentration distribution at 6 and 24 hours after leak initiation and 24 hours after leak termination for Undisturbed Soil under Asphalt pavement, Trench with Pipe under Asphalt pavement, Trench with Moist Soil under Asphalt pavement, and Trench with Pipe Moist soil and Pipe under Asphalt pavement experiments. (a), (d), (g), (j), and (b), (e), (h), (k) are vertical profiles for 6 and 24 hours respectively after leak initiation. (c), (f), (i), (l) are vertical profiles for 24 hours after leak termination. The respective belowground profile key for each experiment, the location of the leak point, measurement points, and the asphalt layer are also shown. Surface and subsurface measurement points are shown in black and white dots respectively. Profiles are created considering a homogeneous soil structure along all directions.....	54
Figure 13: Variations in (a) Belowground flammable threat zones based the on belowground location of the 5% and 15% CH <sub>4</sub> (v/v) contours and (b) Belowground methane-contaminated zone based on the belowground location of 0.01% CH <sub>4</sub> (v/v) contours. The overall migration rates are also shown. Here the location and migration rates are shown for both the active leak period and after leak termination.....	55
Figure 14: Belowground Vertical and horizontal CH <sub>4</sub> profiles for a 10 slpm NG leak under unpaved undisturbed dry soil conditions.....	57
Figure 15: Belowground Vertical and horizontal CH <sub>4</sub> profiles for a 10 slpm NG leak under undisturbed near surface moist soil conditions.....	58
Figure 17: Integrated simulation domain representing soil matrix, leak point, surface and subsurface complexities, and boundary conditions.....	62

- Figure 17: Variation in relative maximum migration distance ( $D_{max}$ ) by  $CH_4$  plume boundary, 5%, 15%, 20%, and 30%  $CH_4$  (v/v) contours for a 1 slpm leak at 0.1 m depth (a) 24 hours, (b) 2 weeks, (c) 2 months, after leak initiation and at 0.9 m depth (d) 24 hours, (e) 2 weeks, (f) 2 months, after leak initiation under different surface, and subsurface complexities. Here  $S_w=50\%$  represent that the soil is 50% moisture saturated. Vertical black line is the “unit” indicator for the basecase..... 63
- Figure 18: Variation in relative maximum migration distance ( $D_{max}$ ) by  $CH_4$  plume boundary, 5%, 15%, 20%, and 30%  $CH_4$  (v/v) contours for a 10 slpm leak at 0.1 m depth (a) 24 hours, (b) 2 weeks, (c) 2 months, after leak initiation and at 0.9 m depth (d) 24 hours, (e) 2 weeks, (f) 2 months, after leak initiation under different surface, and subsurface complexities. Here  $S_w=50\%$  represent that the soil is 50% moisture saturated. Vertical black line is the “unit” indicator for the basecase..... 64
- Figure 19: Variation in migration rate range by 0.5%, 5%, 15%, 20%, and 30%  $CH_4$  (v/v) contours for a 1 slpm leak at 0.1 m depth (a) 24 hours, (b) 2 weeks, (c) 2 months after leak initiation and at 0.9 m depth (d) 24 hours, (e) 2 weeks, (f) 2 months after leak initiation under different surface, and subsurface complexities. Here, the bottom margin of each color box represents the minimum migration rate, the upper margin represents the maximum migration rate, and the dark line represents the average migration rate shown by each concentration contour under the respective category. Here  $S_w=50\%$  represent that the soil is 50% moisture saturated. .... 66
- Figure 20: Variation in migration rate range by 0.5%, 5%, 15%, 20%, and 30%  $CH_4$  (v/v) contours for a 10 slpm leak at 0.1 m depth (a) 24 hours, (b) 2 weeks, (c) 2 months after leak initiation and at 0.9 m depth (d) 24 hours, (e) 2 weeks, (f) 2 months after leak initiation under different surface, and subsurface complexities. Here, the bottom margin of each color box represents the minimum migration rate, the upper margin represents the maximum migration rate, and the dark line represents the average migration rate shown by each concentration contour under the respective category. Here  $S_w=50\%$  represents that the soil is 50% moisture saturated. .... 67
- Figure 21: Variation in subsurface 0.5%, 5%, 15%, 20%, and 30%  $CH_4$  (v/v) contour migrations over time at 0.1 m and 0.9 m depths from a 1 slpm leak under different surface and subsurface complexities..... 68
- Figure 22: Variation in subsurface 0.5%, 5%, 15%, 20%, and 30%  $CH_4$  (v/v) contour migrations over time at 0.1 m and 0.9 m depths from a 10 slpm leak under different surface and subsurface complexities..... 69

## **List of Tables**

Table 1: Tested parameters under the experimental method for understanding subsurface migration patterns of leaked natural gas.....	27
Table 2: Leak scenarios selected for numerical simulations and the related surface and/or subsurface complexities.....	29
Table 3: Summary of the experiments conducted to collect data sets including the experiment dates, parameter considered, leak depth, leak rate, gas composition, surface-subsurface condition, and water saturation.....	44

## **List of Acronyms**

AM-2 – Airfield Matting  
BGS – Blow Ground Surface  
CFD – Computational Fluid Dynamics  
CFDM – Computational Fluid Dynamics Model  
CGI – Combustible Gas Analyzer  
CNG – Compressed Natural Gas  
CSU – Colorado State University  
ESCAPE – Estimating the Surface Concentration Above Pipeline Emissions  
HAZMAT – Hazardous Materials  
IAB – Industry Advisory Board  
INIR – Integrated Infrared  
LADR – Leak Detection and Repair  
LEL – Lower Explosive Limit  
ME – Methane  
METEC – Methane Emissions Technology Evaluation Center  
NG – Natural Gas  
PHMSA – Pipeline and Hazardous Materials Safety Administration  
PPE – Personal Protective Equipment  
PRCI – Pipeline Research Council International  
PTFE – Polytetrafluoroethylene  
PVC – Polyvinyl Chloride  
RP – Response protocol  
SCFH – Standard Cubic Feet per Hour  
STP – Standard Temperature Pressure  
SVE – Soil Vapor Extraction  
TAP – Technical Advisory Panel  
UEL – Upper Explosive Limit



# **1. Introduction**

## **1.1 Background and Objectives**

While natural gas (NG) pipeline safety has greatly improved in recent decades (Vetter et al., 2019), leakage incidents still occur due to aging infrastructure, excavation, and human error. While all leaks near structures present some hazard, large and sudden leaks which can quickly migrate through the subsurface and into structures (e.g. basements, foundations, or sewers) are of particular concern. The PHMSA *Significant Incident Consequences Summary* identified that from January 2010 to January 2024, 1434, total incidents were reported, of which 89 of the incidents were fatal causing 132 deaths and 298 incidents causing injuries to 605 individuals (PHMSA, 2024).

Substantial investment has been made in NG sensor technologies in the last 5 years, primarily focused on reducing costs and improving leak detection analytics for aboveground NG infrastructure (Zimmerle et al., 2017). Although recent technological advances in methane detection have improved aboveground leak detection and repair (LDAR) accuracy and efficiency, these improvements do not readily transfer to subsurface leaks from pipelines due to the complex behavior of subsurface gas migration and diffuse presentation of underground leaks. Behavior is influenced by soil layers, subsurface infrastructure, pipeline pressure, and gas composition when pipelines are carrying gas with higher hydrocarbons (C2+). Surface conditions such as pavement, frost, or structures also create barriers to gas flow and release to the atmosphere, increasing lateral transport or causing accumulation below ground (Figure 1). NG migration is also affected by pressure differentials which develop from short-term fluctuation on barometric pressure due to wind variation (Poulsen Tjalfe G. et al., 2003), meteorologically induced long-term changes in barometric pressure (Kesikuru et al., 2001), and water table fluctuations (Patterson & Davis, 2009).

Recent works demonstrate potentially critical limitations of the effectiveness of aboveground leak detection methods for the detection of subsurface NG leaks (Ulrich et al., 2019). In general, aboveground methods do not translate directly to underground NG leaks due to the significant differences in (a) the diffuse presentation of subsurface leaks relative to equipment leak sources, (b) the environmental conditions in the near surface and below the ground surface, and (c) the extended geometry of pipeline systems. To our knowledge, the two analytical tools by Cho et al. (2020) and Riddick et al. (2021) are the first tools, verified by controlled experimentation and numerical modeling, that clearly link key surface environmental parameters to subsurface

migration and leakage rates. However, the above works focused only on steady-state, smaller leaks, characteristic of routine distribution system leak events. Further, our work indicates that larger leaks behave differently during the critical transient phase immediately after leak initiation. The following work addresses this by creating a more complete picture of the large leak behavior necessary to guide first response efforts.

The impact of the aforementioned environmental conditions on gas migration is poorly understood. Analysis of catastrophic leak incidents indicates that the gas may migrate 20 feet or more within thirteen minutes of a large pipeline leak incident (NTSB, 1979). However, first responders have limited tools to estimate the potential zone of migration based upon readily collected measurements at a leak site, such as gas concentration measurements (at or near the surface, or in shallow “pogo stick” holes), observations of the expected leak size, time since leak initiation, and soil conditions. Better understanding of the conditions that increase gas migration distance and speed will support a more efficient response to leaks in general and, ultimately, allow operators and first responders to quickly identify scenarios where gas may migrate extended distances.

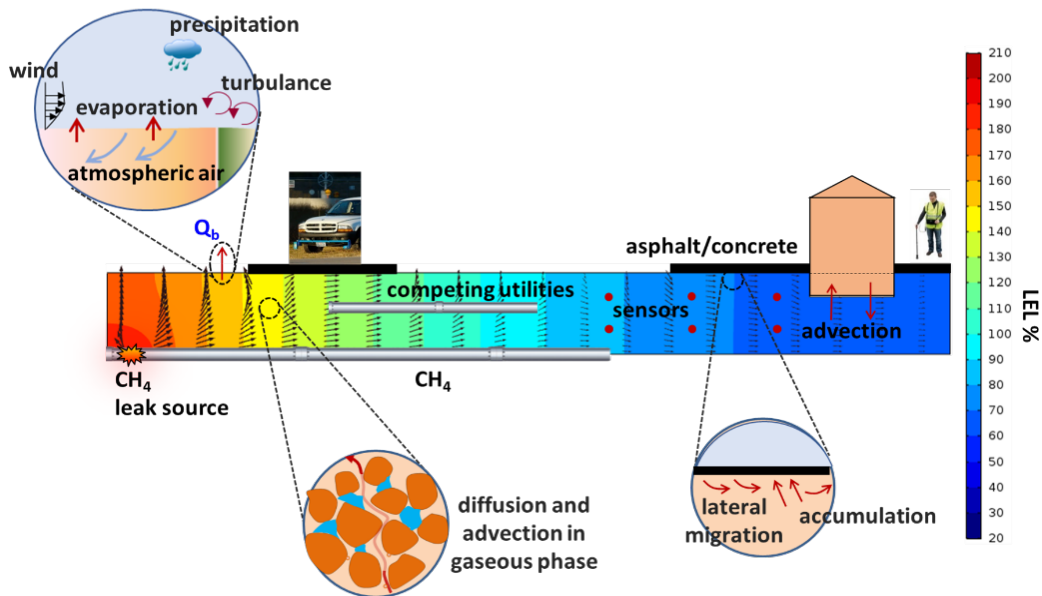


*Figure 1: An idealized schematic of gas leakage from an underground pipeline and the complex mechanisms that affect the gas migration and intrusion into a basement or substructure. Arrows represent gas flow velocity and contour the methane percent of the lower explosive limit. Arrow lengths are proportional to the logarithm of the velocity magnitude. Modelling by PIs.*

Similar unknowns are present in leak venting strategies used to lower underground concentrations after leaks have been identified and stopped. While soil venting systems are simple and installation of bar holes is considered standard industry practice, the design, operation, and monitoring of soil venting systems are non-trivial. In some cases, NG has been vented for long periods without decreasing the soil NG concentration substantially. Incidents such as these are concerning, suggesting two potential problems: (a) these results may indicate that “standard” industry practice does not adapt to local soil conditions and requires substantial trial and error, or (b) these results may indicate that *all* gas leaks have not been identified. The proposed modeling will investigate whether variations in venting strategies (e.g., hole placement, flow rates, and pressure) may impact venting times and efficiencies.

## 1.2 Scope of Work

This project (1) developed experimental methods to measure and understand the transient behavior of significant pipeline leaks, (2) made extensive measurements of appropriately sized leaks, (3) extended measurement using modeling and additional scenarios, and (4) provided updated guidance for first responder and leak detection protocols. Primary tasks included:

**Task 1: Establish a collaborative study structure:** The project used a collaborative governance structure modeled on the team’s prior studies. An active *technical advisory panel* (TAP) was assembled including representative end users of response protocols: first responders, NG operators (distribution and midstream), and regulatory agencies. The TAP provided industry expertise to help the work remain relevant and useful. Two first responders and 10 industry partners agreed to support this study. The team regularly updated and engaged the TAP, as well as the Methane Emission Technology and Evaluation Center (METEC) *Industry Advisory Board* (IAB) which includes industry associations that provide broad outreach to NG operators.

**Task 2: Survey existing first responder operational practices:** The project reviewed existing response protocols (RPs) for significant gas leakage events, starting with the TAP and extending to other organizations. TAP members provided their RPs and the Poudre Fire Authority HAZMAT team also participated in selected leak tests at METEC, allowing the study team to directly observe first responder practices. Analysis of existing protocols built the team’s understanding of leak RPs, provided guidance for project execution, and assisted the incorporation of study results into RP guidance.

**Task 3: Methods Development:** While methods for measuring steady-state underground gas concentrations are well developed, methods to measure underground gas concentration while gas is actively migrating during transient events are not well developed. To meet project requirements, the team developed high-speed, *in situ* measurements: sensor elements introduced into the subsurface that operate effectively in the high-humidity, high-concentration, environment likely to be seen during testing.

Resulting systems can measure gas migration speeds greater than 1 foot per minute using an innovative “sensor-in-sleeve” approach. During testbed construction, tubes were inserted to appropriate depths in the testbed. A specially designed probe was then inserted into the tube just prior to initiation of the test. During the experiment, data acquisition systems on the surface read the sensors using an analog connection sampled at 0.2 Hz. After the experiment, sensors were removed and redeployed for the next test.

**Task 3.1: Sensor Testing:** Sensor testing was completed to characterize stability and accuracy for mid-to-high gas leak events. The study team used sensors that met the required specifications (e.g. stable, low oxygen environment with quick response to concentration changes). Sensors were tested by: (1) in-atmosphere testing using test chambers at METEC to test stability, response rates, and tolerance to high humidity; and (2) comparing to previously observed methods which had produced high-quality results during prior studies at METEC: Mitton (2018) and Ulrich et al. (2019). The sensors were also tested with “wet” gas that includes C2-C4 alkanes using a gas mixing system at METEC.

**Task 3.2: Installation of Test Sensors at METEC:** The team built two underground testbeds to accommodate gas flows of 10 – 300 slpm (20 – 600 scfh) by installing larger tubes, flow meters, and modifying overburden thickness to prevent premature structural failure during high flow rates (i.e. cracking of the ground from leak location to surface).

Three underground structures (6’ x 6’ basement, concrete slab, crawl space) were constructed 15 ft distance from the release points to simulate the gas ingress into substructures. Structures were designed to operate in two modes: (a) as loosely sealed chambers with little to no atmospheric air exchange, and (b) in a semi-ventilated mode, simulating the air exchange common for basements.

Since the underground structures intentionally disrupt gas migration patterns, release points were installed 3 ft deep and 15 ft away from the structures. Release points were implemented similarly to other METEC testbeds (Mitton, 2018) – stainless steel tubing terminating in a gravel-

filled enclosure (to prevent plugging) at the release point. Release points, sensor tubes, and structures were installed, and the ground was allowed to settle prior to testing. Gas meters and data acquisition equipment were housed in existing METEC structures.

**Task 3.3: Document Method:** Developed methods were documented in project reports and/or journal articles in sufficient detail to be usable by the other researchers.

**Task 4: METEC Experiments:** Primary testing for the study was performed for 12 months at METEC to include a range of weather conditions (particularly wind and barometric pressure changes), surface covers (e.g. snow, moist topsoil or impermeable covers created using portable airfield aluminum matting (AM2) on loan to METEC from the U.S. Air Force), and subsurface conditions (e.g., soil disturbance, buried infrastructure). In total, 150 experiments for leak rates ranging from 10 – 200 slpm (20 – 400 scfh) were conducted.

**Task 5: TTC Experiments:** This task was removed from the final contract and is retained here to maintain task numbering from the original proposal.

**Task 6: Extend Results via Modeling:** In unison with experiments, numerical simulations were performed using computational models to guide observations and interpret data. Numerical simulations were performed using the multiphase transport simulator COMSOL Multiphysics® (Gao et al., 2020; Jayarathne et al., 2023). The model simulated the transport of aqueous and gas phases containing multi-components under non-isothermal conditions. Using the numerical model, the study varied environmental conditions more widely than can be done experimentally, allowing for over 1000 simulations of different environmental and operating conditions. The model was also used to do a limited exploration of soil aeration methods. Soil aeration simulations allowed for ‘proof of concept’ understanding of the impact in bar hole placement, and venting pressures on effective gas removal strategies.

**Task 7: Develop recommended practices on development and dissipation of leaks with significant flow rates:** Results of tasks 2-6 were used to establish guidance that can be translated into recommended practices by relevant standard organizations, PHMSA, or state agencies. This task included multiple rounds of consultation with the TAP, during which the study team interacted with the TAP, acquired feedback, and edited the guidance document.

**Task 8: Final Reporting:** The project plan included a final task to complete reporting and journal publications.

## **2. Deliverable 2: Survey existing first responder operational practices**

### **2.1 Objectives**

Survey existing RPs for significant gas leakage events, starting with the TAP and extending, as necessary, to other organizations. Analysis of existing protocols will build the team's understanding of leak response procedures, guide project execution, and assist in incorporating study results into future RP guidance.

### **2.2 Activities**

Preliminary TAP members provided their RPs. Details related to this deliverable can be found under Appendix 1: Survey of first responder operational practices: Current understanding of first responder operational practices when responding to large pipeline leak events.

### **2.3 Observations**

PHMSA guidelines state that first responders' safety and the safety of the community is the top priority for emergency first responders attending natural gas pipeline leakage events (PHMSA, 2020). A first responder can include both emergency first responders (fire fighters, police, and paramedics) and gas company employees (including contractors employees working for the operator, and workers on the right-of-way). Both PHMSA and local fire authority operational directives state that first responders' arrival at a pipeline incident should include coordination with operators, shutting off gas supplies, and various important safety activities, one of which is to determine if and where the atmosphere is hazardous, defined as total hydrocarbon concentration (TCH) in an enclosed or open space exceeding 10 and 20% LEL, respectively (PHMSA, 2016; Pipeline Emergency Response Guidelines, 2018; Poudre Fire Authority, 2019). First responders use Combustible Gas Indicators (CGIs) to determine the maximum total hydrocarbon concentration (THC), thereby providing information to properly establish setback distances from the high concentration locations. Should an elevated reading be recorded, first responders establish a 'Hot zone', defined as a setback radius of 300 feet for gas leaks or 150 feet for liquid leaks. From first responder's protocols, action is only taken when the THC at the ground surface reaches 5,000 ppm (10% LEL), the THC within a building exceeds 500 ppm or if an excavated and measured leak exceeds 10 scfh (~200 g h<sup>-1</sup>; ~5 slpm). What is not clear is what these values imply about the size of the leak and how this could change with different environmental conditions. For

an event where the maximum THC concentration is less than 10 % LEL indoors or 20% LEL outdoors, the response is at the discretion of the response lead and there are no set protocols.

In the review of first responder pipeline emergency response guidelines and local fire authority operational directives, some acknowledgement of the impact of the environmental and pipeline operating conditions on the leaked gas behavior exist (Blankinship et al., 2008; Hildebrand & Noll, 2017; National Volunteer Fire Council et al., n.d.; *Pipeline Emergency Response Guidelines*, 2006). Examples include:

- “Natural gas can be trapped under asphalt, concrete, or frozen ground and move laterally from its source in underground conduits, casings, and rights of ways.” (Blankinship et al., 2008, National Association of State Fire Marshals)
- “Natural gas leaks can produce a situation where product may filter through soil, follow storm drains, sewers, water lines, or other utilities and then emerge some distance from the actual leak site.” (NVFC and USDOT PHMSA (2018), ICS-204)
- “One concern is the ability of gas leaks to migrate through the soil, follow water and sewer lines, or collect in storm drains. Since interstate pipelines often transport their products without an odorant added, the sense of smell is not a reliable indicator of the presence of gas. It’s important to remember that even in pipelines or distribution systems where odorants are added, methyl mercaptan is heavier than natural gas and may not make it to the surface level when gas is migrating.” (NVFC and USDOT PHMSA (2018), ICS 215A)
- “Natural gas is lighter than air and will rise.” (USDOT PHMSA, 2018)
- “Underground leaks of natural gas will follow the path of least resistance. Soil that has been disturbed by excavation will allow for the easier passage of natural gas. In addition, certain soils may cause the mercaptan odorants to be “scrubbed” from the natural gas.” (USDOT PHMSA, 2018)
- “Pipelines contain flammable . . . gases that present emergency responders with a myriad of hazards and risks that vary depending on the topography, weather, and properties of the material involved.” (Pipeline emergency response guidelines, 2018)

Although the general impact of the environment (e.g. topography, weather, and pipeline properties) are acknowledged in first responder literature, how to incorporate any knowledge of

this impact into practice is limited, if not missing. For example, when establishing the exclusion zones, PHMSA recommend using the following information, even though there is no quantitative guidance on how exclusion zones are to be calculated:

- Pressure and diameter of pipe.
- Timing of valve closure by the pipeline operator.
- Dissipation time of the product in the pipeline once valves are closed.
- Ability to conduct atmospheric monitoring and/or air sampling.
- Weather (wind direction, etc.).
- Local variables such as topography, population density, demographics, and available fire suppression methods.
- Nearby building construction material/density.
- Natural and man-made barriers (highways, railroads, rivers, etc.).

## **2.4 Key findings**

- Both emergency responders and gas distribution companies have clearly defined roles when attending gas leak events. The top priority is to protect the public by stopping the gas supply, establishing safe zones, methodically checking houses for explosive concentrations, and evacuating people as necessary.
- In the review of first responder pipeline emergency response guidelines and local fire authority operational directives, some acknowledgement of the impact of the environmental and pipeline operating conditions on the leaked gas behavior exist. However, how to incorporate any knowledge of this impact into practice is limited, if not missing.
- Although PHMSA recommends that exclusion zones should account for weather conditions, this is not generally considered by first responders because there is no reliable, easily implemented, quantitative guidance that connects weather conditions to risk.
- The principal cause of fatality for the public is structural explosions and fire. In approximately 70% of the fatality cases, the explosion is the first sign of a leakage



event, and first responders are only alerted after the incident. The remaining 30% of structure explosions happened 30 to 200 minutes after first responders arrived on site. In these cases, a better understanding of gas migration and speed would better inform first responders of which structures were most at risk for fire or explosion.

- Considering the 30% of cases where first responders have time to respond, if the speed of gas migration can be estimated from environmental variables, it may be possible for first responders to develop better estimates for the necessary evacuation zone. This would reduce risk without creating excessively large evacuation zones. Additionally, these calculations would generally inform first responders of how environmental conditions impact the risk level for a specific leak condition.

### **3. Deliverable 3: Methods for estimating gas migration and leak size from readily obtained measurements at a leak event**

#### **3.1 Objectives**

To advance techniques to experimentally measure transient belowground gas migration from mid- to large-sized leaks in real time. A medium is defined as 2.2 – 35.4 slpm (4.7 – 75 scfh) and a large leak is greater than 35.4 slpm (75 scfh).

#### **3.2 Activities**

Further details can be found at Jayarathne et al. (2022, 2023, 2024), Appendix 3: RPLUME/ UPSIDE Data Management Protocol, Appendix 5: Understanding of the degree to which parameters affect the subsurface natural gas migration with significant flow rates: Experimental Report, and Appendix 6: Understanding of the degree to which parameters affect the subsurface natural gas migration with significant flow rates: Simulation Report.

#### **3.3 Experimental Method**

The method consists of field tests using below- and aboveground sensors to characterize gas migration speed and distance. Experiments used significant leak rates defined as:

- Medium size: 2.2 – 35.4 slpm (4.7 – 75 scfh)
- Large size: > 35.4 slpm (75 scfh)

From previous experimental and simulated studies on emissions of smaller leak rates (Gao et al., 2021; Ulrich et al., 2019), factors that affect NG subsurface migration speed and distance are soil structure, subsurface infrastructure, pipeline pressure, gas composition, frost or structures that create barriers to gas flow, surface covers, and environmental conditions (near-surface wind, temperature, and precipitation). The parameters tested in these controlled release experiments are listed in Table 1. Additionally, a range of environmental conditions were covered during the experiments.

*Table 1: Tested parameters under the experimental method for understanding subsurface migration patterns of leaked natural gas.*

<b>Parameters</b>	<b>Range tested</b>
NG Leak rate	21 – 424 scfh (10 – 200 slpm)
Gas Compositions	Methane 85%, Air 15% - Baseline characteristic
	Methane 70%, Ethane 30%
	Methane 70%, Ethane 20%, Propane 10%
Soil moisture	25% - 49% by volume
Surface conditions	Uncovered – Baseline characteristic
	Snow cover
	Asphalt cover
	Moisture cap (Saturated layer of soil near the surface)
	Impermeable covers simulating a driveway, walkway, and patio cover
Subsurface complexity	Buried empty pipeline/conduit
	Disturbed soil (Trench)

Experiment methods utilized two testbeds designed for these experiments. Testbeds include a network of belowground CH<sub>4</sub> concentration, soil, and atmospheric sensors to continuously monitor the test sites. Belowground CH<sub>4</sub> concentration was continuously measured and logged at 5-second time intervals. Soil environmental sensors (Appendix 3) were used to continuously measure soil moisture, temperature, and matric potential at 10-minute intervals. Atmospheric variables were measured in 30-second intervals using local weather stations located at 0.05, 0.5, 1 and 10 m heights from the soil surface. Belowground NG releases occurred for 24 hours for releases below 100 slpm (212 scfh), and for 6 hours for releases of 100 and 200 slpm (212 and 424 scfh respectively). For the smaller leaks, the release period of 24 hours covered the influence of diurnal variation in atmospheric conditions which would typically occur before the leak was discovered. In contrast, the 6-hour periods for large leaks represent typical leak duration prior to response from taken from PHMSA incident reports (Appendix 1).

The method continued measurement up to 12 days after stopping the gas supply (leak termination) to properly capture the soil venting patterns. Note that all venting in these experiments was natural venting; no bore holes or forced air venting was used.

In general, the experimental process was:

1. Sensors were installed as described above.
2. Sensors were recorded for hours to days to establish a stable background concentration.
3. The leak – i.e. gas flow – was initiated.
4. During active gas flow:
  - a. All underground sensors were monitored continuously to develop a concentration time series. In addition to gas concentration, soil moisture, pressure, and temperature were also monitored using sensors installed throughout the testbeds.
  - b. The surface plume expression was monitored using surface concentration instruments.
  - c. Atmospheric concentrations were monitored downwind during selected experiments.
5. The gas flow was stopped.
6. Underground monitoring continued to determine when the testbed returned to background concentrations, i.e., to determine the concentration variations during venting under each test parameter.

### **3.4 Numerical Method**

The numerical method consists of computational models performed using the multicomponent, multiphase transport simulator COMSOL Multiphysics® 6.1 (hereafter referred to as COMSOL 6.1), which simulated the transport of multiple aqueous and gas phase components under non-isothermal conditions. The numerical model allowed exploration of parameter combinations beyond experimentally measurable scenarios. The numerical method was used to develop estimates of migration distance and migration rate under various parameter combinations.

Simulation scenarios were selected to represent 1) leaks under different soil types, 2) leaks under soil-moisture saturations, 3) leaks under different surface conditions, 4) leaks associated with different subsurface anomalies, and 5) leaks associated with different surface and subsurface complexity combinates as shown in Table 2.

Table 2: Leak scenarios selected for numerical simulations and the related surface and/or subsurface complexities.

Simulation No.	Simulation Scenario Name	Complexity Description	Complexity Category
1	Dry Undisturbed Loam	Unpaved undisturbed dry loam soil	Baseline Scenario
2	Dry Sand	Unpaved undisturbed dry sand	Soil Type
3	Dry Clay	Unpaved undisturbed dry clay	
4	Loam (Sw = 50%)		
5	Sand (Sw = 50%)	A moisture profile with 80% saturation at the surface	Soil Moisture Saturation
6	Clay (Sw = 50%)		
7	Short Asphalt Cover	Paved surface	Surface Complexity
8	Long Asphalt Cover	Paved surface	
9	Moist soil layer	Venting condition change due to surface cover	
10	Snow Cover	Venting condition change due to surface cover	
11	Trench	Disturbed soil	Subsurface Anomaly
12	Trench Moist soil	Disturbed partially saturated soil	
13	Fracture / Pipe	Subsurface fault	
14	Trench with Fracture	Integrated disturbed soil and subsurface fault	
15	Trench Short Asphalt	Disturbed soil with paved surface	Combined surface and subsurface complexities
16	Trench Long Asphalt	Disturbed soil with paved surface	
17	Trench/Fracture Short Asphalt	Disturbed soil, subsurface fault with paved surface	
18	Trench/Fracture Short Asphalt	Disturbed soil, subsurface fault with paved surface	
Dry - Soil moisture saturation is 25%		Sw = 50% - Soil moisture saturation is 50%	

### 3.5 Selection of a Baseline Scenario

The project focused on NG migration for “significant” leaks. To facilitate comparison, the project defined a baseline leak rate of 10 slpm (20 scfh). The baseline testbed configuration was defined as grass-covered native soil with no additional subsurface complexity (e.g. other underground pipes or conduits). The baseline releases used distribution grade NG (mixture of 85±2 % CH<sub>4</sub> v/v).

To maintain the consistency with the experimental method, the baseline scenario for the numerical simulations was also a leak rate of 10 slpm (20 scfh), gas composition of 85% CH<sub>4</sub> v/v and 15% air v/v, and dry soil with neither surface cover nor subsurface complexity. Based on guidance from the TAP, the leak rate for modeling scenarios was lower, ranging from 2-20 scfh (1-10 slpm), thus allowing for the simulation of longer time periods in addition to the short term, transient gas behavior.

### 3.6 Comparison Matrices

The effect of each parameter was determined by comparing the belowground CH<sub>4</sub> concentrations at specific distances to the baseline scenario. Since gas concentration is a continuum, it is convenient to compare the location and time of arrival for specific CH<sub>4</sub> concentration values between experiments and the baseline scenario. The selected CH<sub>4</sub> concentrations for the comparison were:

- Upper explosive limit (UEL) of methane (15% of CH<sub>4</sub> v/v or 150,000 ppm)
- Lower explosive limit (LEL) of methane (5% of CH<sub>4</sub> v/v or 50,000 ppm)
- 10% of LEL (0.5% of CH<sub>4</sub> v/v or 5,000 ppm); chosen as it marks the minimum CH<sub>4</sub> limit for evacuations during a leak event
- 20% and 30% CH<sub>4</sub> were also used for the numerical simulations, based on CH<sub>4</sub> indications used by industry to classify leaks into different grades (see response guidance document)

Based on the selected concentration contours, two comparison matrices were created as follows:

1. Maximum horizontal distance that 10% LEL, LEL and UEL travelled
2. Average migration rate of 10% LEL, LEL and UEL

The horizontal distance to the farthest sensor (for experiments) or the location (for simulations) that recorded explosive limit concentrations (10% LEL, LEL and UEL) from the release point was taken as the maximum distance. The average migration rate was calculated by dividing the maximum distance traveled by the time taken to reach the sensor for the first time (Equation 1).

$$\text{Average Migration rate} = \frac{\text{Maximum horizontal distance (m)}}{\text{Time taken to reach maximum distance for the first time (hr)}} \quad (1)$$

It is important to note that the LEL and UEL gas concentration values utilized here represent the gas concentration *in the soil*. These values are not generally comparable to, or indicative of, LEL or UEL concentrations in a structure positioned in or on the soil. Specifically, the gas concentration and gas composition in the soil may be different than the gas concentration in a structure.

## **4. Deliverable 4, 5: Testbed completion and measurement points installment**

### **4.1 Objectives**

Develop an experimental site resembling real world belowground NG pipeline leakages from distribution lines. The site should also be able to create different environmental conditions in a residential area and be able to measure belowground NG and environmental variables temporally and spatially with a high resolution.

### **4.2 Activities**

Two testbeds were designed and built at the Colorado State University (CSU) Methane Emission Technology Evaluation Center (METEC) in Fort Collins, CO. The testbeds allow for the simulation of underground pipeline leaks at known leakage rates in varying subsurface and surface conditions, allowing for both control and measurement of subsurface and surface conditions on a continuous basis. A “rural” testbed was designed to investigate gas transport from gathering pipelines in a rural environment with undisturbed soil. An “urban” testbed was designed to test how NG will travel in urban and suburban environments. Urban/suburban environments were simulated using impermeable coverings (roads/driveways), semipermeable covering (gardens) and closed subsurface conduits (representing empty pipelines or conduit such as sewer or telecommunication lines). The urban environment was simulated using selectively open conduits and impermeable coverings (roads). The testbeds were instrumented with a variety of subsurface, surface, and atmospheric sensors to continuously monitor the gas and environmental conditions as described earlier. Further details can be found under Appendix 2: Performance Testing of SGX Integrated Infrared (INIR) sensor in subsurface methane detection and Appendix 3: RPLUME / UPSIDE Data Management Protocol.

### **4.3 Rural Testbed**

The testbed consists of emission points located at two depths belowground – 0.9 m (3 ft) and 1.8 m (6 ft) – and over 70 belowground, surface, and atmospheric sensors to capture both the gas concentration and environmental conditions. Gas is supplied by 0.635-cm (1/4”) polytetrafluoroethylene (PTFE) tubing and released via a 0.635-cm vent screen (model SS-MD-4,



Swagelok, USA) surrounded by a 10-cm (4”) wire cube filled with gravel to prevent clogging. Compressed NG with methane compositions ranging from 85 to 95% v/v methane are provided from two 145-L (5 cu ft) cylinders and controlled using pressure regulation and solenoid valves in series with precision choked flow orifices. Each emission point is capable of releasing between 10 – 300 splm (20 – 600 scfh). All subsurface methane concentrations in the rural testbed were continuously measured at 30 belowground locations (Figure 2) using SGX INIR-ME 100% sensors (SGX, Katowice, Poland). The sensors have a detection limit of 100 ppm, capable of measuring up to 100% concentration. Sensors were installed at 0.9 m (3 ft) , 0.6 m, and 0.3 m (3 ft, 2ft, and 1 ft respectively) below the surface at distances 0.9 m (3 ft) , 1.8 m 3 m, 4.5 m, 15 m, and 30 m (3 ft, 6 ft, 10 ft, 50 ft, and 100 ft respectively) from the leak point as shown in Figure 2.

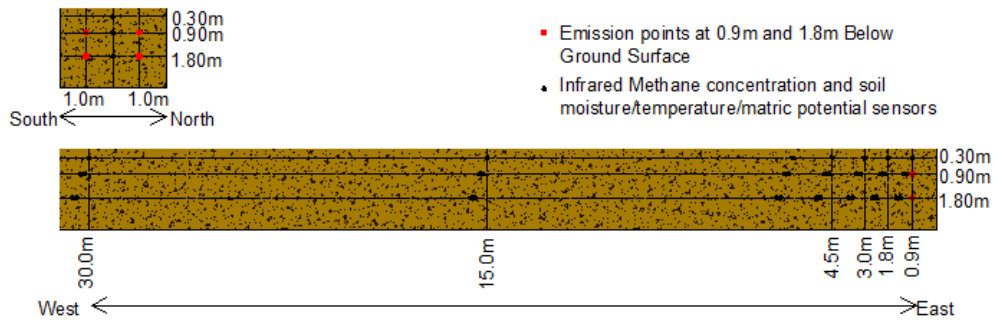


Figure 2: Schematic of the rural testbed profile with locations for belowground Emission points and sensor locations for methane (INIR-type) and soil moisture/temperature/matric potential sensors. Specific distances from the emission point and depths from the surface are also shown.

#### 4.4 Urban Testbed

This 100 m (330 ft) long and 15 m (50 ft) wide testbed consists of three identical structures positioned on three different foundation types: basement, crawlspace, and slab-on-grade. The three structures (1-3) are wooden sheds with footprints identical to their foundations. The basement consists of a 0.9 m (3 ft) deep, 0.1 m (4 inch) thick 1.8 x 1.8 m (6 x 6 ft) concrete floor and cinder block walls. The crawlspace consists of a single layer of standard-size 8-inch cinder blocks. The slab-on-grade concrete is a 0.1 m (4 inch) thick, 1.8 x 1.8 m (6 x 6 ft) slab set on the ground. The three structures are located far enough from each other so that releases at one structure will not interfere with releases from another.

The area around each structure includes two NG release points located 0.9 m (3 ft) below ground surface (BGS), and 5.5 m (18 ft) away from the edge of the foundation (Figure 3). The depths were selected based on soil cover requirements for NG distribution mains which range from 24 to 48 inches, depending on the type, class, and location of the pipeline (Electronic Code of Federal Regulations §192.327 Cover, 2021).

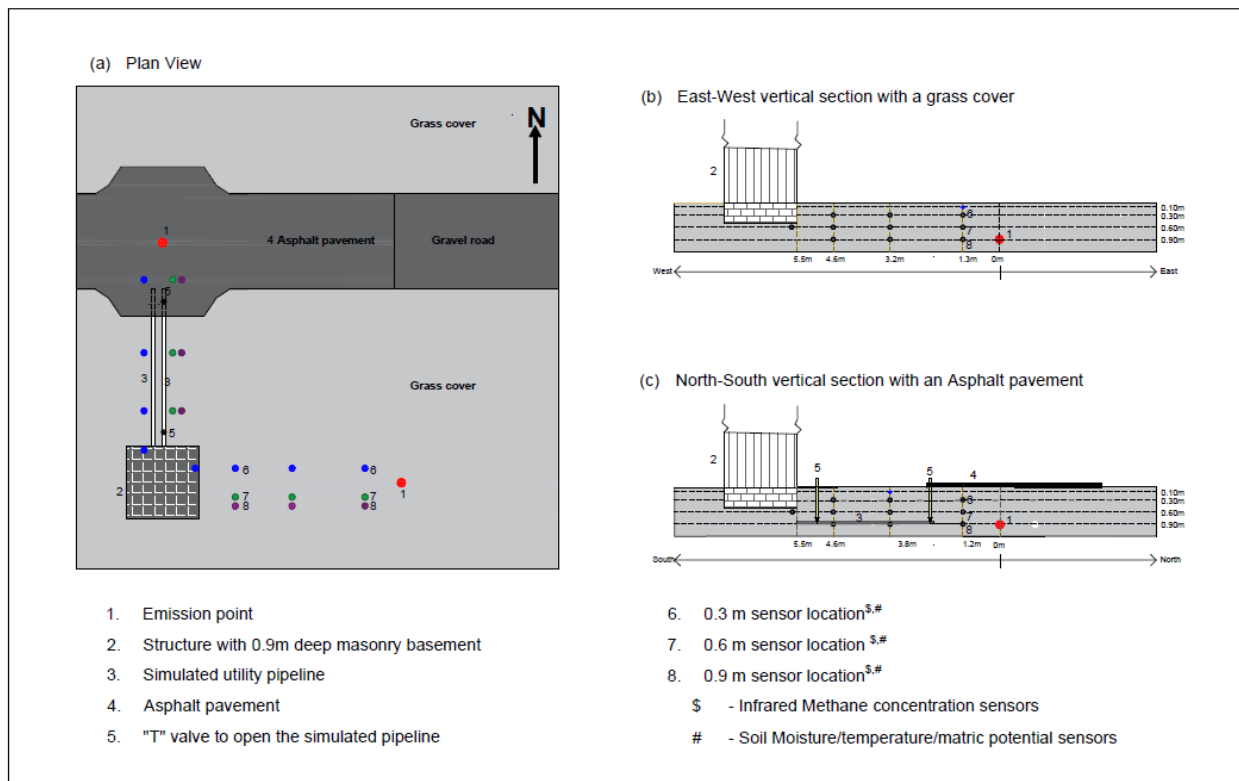
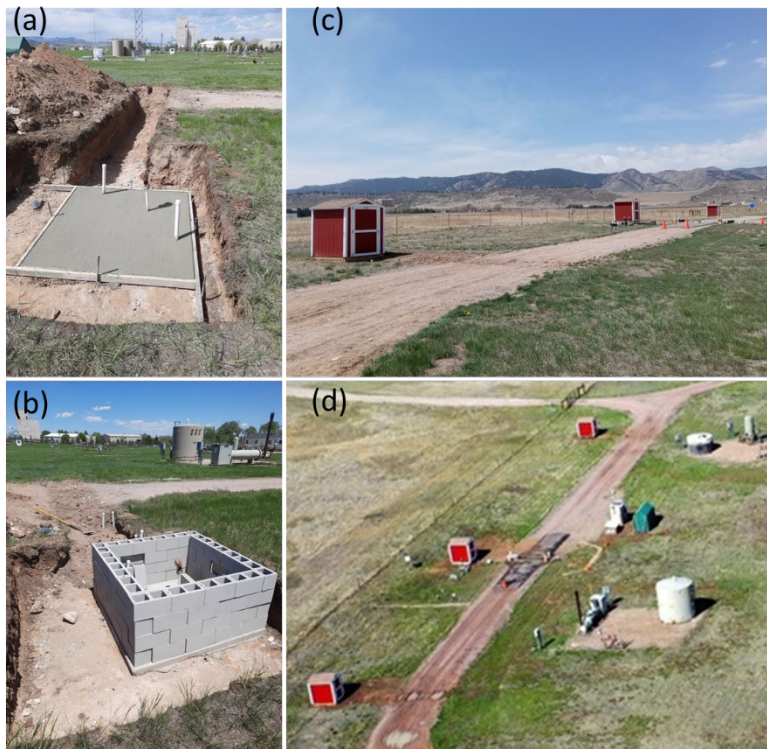


Figure 3 Schematic of the testbed profile for the structure with a basement. (a) Plan view of the testbed with the basement structure (b) East-West profile with a grass cover and (c) North-South profile with an asphalt pavement. Location of gas release points, sensor locations, the utility pipelines, and the location for each type of sensors are also shown.

To simulate urban and suburban subsurface environments, two buried utility conduits were installed at a depth of 0.9 m (3 ft) running from the road – located 5 m (16 ft) from the structures – towards the structure (Figure 4). One 0.05-m (2-in) diameter pipe has a valve at both ends and can be selectively opened or closed to simulate an empty communication or sewer line (urban environment) or a sealed pipe (suburban environment). A 0.1-m (4-in) diameter pipe, sealed at both ends, was laid alongside the first to simulate gas migration along the disturbed soil surrounding the pipe. Belowground installation was performed similarly to commonly practiced

pipeline installation procedures. Soil was trenched 0.3 m (12-in) wide and 0.9 m (3 ft) deep, pipe was laid in the trench, and backfilled with native soil. Soil was compacted using a vibratory compactor and then allowed to settle naturally over time.

A 2.3 m (7.5 ft) wide and 15 m (50 ft) long asphalt paved road was laid 5 m (16 ft) from the structures (Figure 4). In addition to asphalt, other movable surface coverings were used, including semi-permeable artificial grass (AstroTurf) and movable impermeable AM-2 matting. AM-2 matting consists of interlocking steel rectangles coated with an epoxy nonskid material that can be assembled in a brickwork pattern to form different surface configurations (e.g., sidewalk) that can be configured in accordance with each experiment.



*Figure 4: Construction of (a) slab-on-grade and (b) basement foundations for structures, PVC sleeves for CH<sub>4</sub> concentration sensors, and the trench running from the structures towards the road are also visible. (c) ground view and (d) aerial view of the completed Urban testbed with three structures, and the asphalt pavement in front of the middle structure.*

A network of methane concentration and soil environmental sensors were used to continuously monitor the belowground CH<sub>4</sub> variations, soil moisture content, soil temperature, and the matric potential. To measure CH<sub>4</sub> variations, 19 SGX INIR-ME100 methane concentration

sensors (Appendix A.3) were deployed underground at 0.3, 0.6, 0.9 m (1, 2, 3 ft) belowground along the vertical sections 1.3, 3.2, 4.6, and 5.5 m (4, 10.5, 15 ft) away from the release point (Figure 2, 3). Soil environmental sensors were co-located with INIR sensors during the installation to accurately measure the environmental parameters at each point.

Prior experimental results and numerical models were used to determine the optimal sensor placement to capture the movement of the belowground NG plume. Two additional sets of sensors were installed underneath the foundation. All environmental sensors are installed permanently while the methane sensor installation is semi-permanent, allowing for periodic removal for calibration, as described earlier.

#### **4.5 Controlled Releases**

NG was supplied to the testbed from the city gas supply as compressed natural gas (CNG) and stored in tanks located onsite. The composition of the gas was determined prior to each experiment using a gas sample analyzed by gas chromatography. When required, a gas mixing rig available at METEC was used to modify the composition of the NG by adding additional methane, ethane, propane, or butane. In these cases, gas composition was calculated using the gas chromatography output for the CNG and adding the mass flow rate of other gases.

The flow from the cylinders was controlled using pressure regulation and on/off solenoid valves in series with precision choked flow orifices. The mass flow rate was controlled using pressure regulation and controlling which solenoid valves were open. While the orifices control the flow rate, actual flow was monitored using either a 0-15 slpm (0-32 scfh) or 0-75 slpm (0-159 scfh) mass flow meter (Omega FMA1700 series). Meter selection was based on the experimental flow rate to maximize the meter's operational span. All control systems are housed in a small structure (i.e., a gas house) near the testbed. Gas houses are insulated to maintain controlled conditions for the flow meter and control equipment during weather extremes.

## **5. Deliverable 6: Approaches to the design, operation, and monitoring of natural gas soil venting systems**

### **5.1 Objectives**

Although natural gas soil venting systems are not the focus of this project, a limited “proof of concept” study was performed to better understand the current use of such system for soil gas aeration and how numerical models can be used to assist in their design. Soil venting or aeration is a practice used by operators to quickly mitigate the presence of elevated concentrations of underground natural gas (NG). While soil venting technology is simple and installation is considered standard industry practice, a limited study focused on the design, operation, and monitoring of soil venting systems for NG removal below the ground is warranted. Thus, the objectives of this work were to (1) review reports, studies, and models applicable to soil venting, allowing us to better understand the current state of industry practice as well as the applicability of a wider body of knowledge to practice, and (2) use selected models to investigate the influence of variation in venting times with changes in soil venting strategies (e.g. bar hole configurations). For additional details, please refer to Appendix 4: Support information for the soil venting system.

### **5.2 Current state of practice**

Soil aeration, which is used to extract elevated gas concentrations from contaminated soil with volatile compounds, is commonly used in the NG pipeline safety for the removal of residual NG due to a pipeline leak event. In standard practice, the soil aeration consists of one or multiple venting bar holes which allow for the natural escape of gas from the subsurface to the atmosphere, thus decreasing belowground concentrations. Depending on the operational constraints, a vacuum or blower is sometimes installed on the bar holes to generate the advective airflow through the soil to decrease the time needed to lower the gas concentration below the approval concentration. Nevertheless, current operations of soil aeration indicate that insufficient aeration and mismatched system configurations or components can impede gas escape and result in incomplete aeration and result in costly cleanup efforts. For example, in Georgetown, TX, NG was vented from an underground leak for more than 30 days without decreasing the soil NG concentration within the non-hazardous level (City of Georgetown Texas, 2019). Reasons the venting may have failed include:

- The installation and operation of the soil aeration did not match local soil gas conditions, resulting in inadequate pathways for the gas to migrate to the venting bar holes and thus escape from the subsurface into the atmosphere.
- There were multiple leak locations replenishing gas in the venting area.
- Some other factor caused gas to migrate into the venting area, causing a rebound of residual gas concentration.

Therefore, while soil aeration processes are considered simple and installation is considered standard practice, the design, operation, and monitoring in the soil aeration practice become a critical and crucial study.

### **5.3 Selected soil venting model**

A previously developed two-dimensional soil venting model was amended and used for this work. The two-dimensional soil aeration model is based on the work of Deepagoda et al. (2016) and Gao et al. (2021), which was previously validated by both lab and field experiments. The model considers two phases (liquid and gas) and two components (CH<sub>4</sub> and air) as incompressible fluids. The soil water was assumed to be immobilized due to the dry soil condition. The air in the model consisted of 86% CH<sub>4</sub>. The dissolution of CH<sub>4</sub> in soil water is neglected due to the assumption of its low solubility in water (0.022 mg/mL). Details of the model can be found in Appendix 4.

### **5.4 Preliminary simulations**

This study focused specifically on the impact of three design criteria: (1) venting pressure, (2) soil type, and (3) barhole configuration. Figure 5 illustrates the variations in residual CH<sub>4</sub> concentrations at the bottom of the venting bar hole in one and three venting bar hole scenarios with six different soil types and venting pressures of 0, 0.2, and 0.5 atm. Soil properties (e.g., porosity and permeability) of each soil can be found in Appendix 4. In the scenario of one venting bar hole with the venting pressure of 0 atm (i.e., without the venting), a similar decrease in residual CH<sub>4</sub> concentration at the bottom of the venting bar hole is observed across all soil types, dropping from 3,300 ppm to 550 ppm on average over a 60 minute period (Figure 5a). However, as venting

pressure increases to 0.5 atm (Figure 5b), soils with high relative permeability (coarse sand) exhibit a noticeable decrease in residual CH<sub>4</sub> concentrations compared to low permeable soils like clay and loam. The residual gas concentrations in the coarse sand were below 50 ppm, which is a standard of stopping soil venting in the operator’s practice, after 7 mins of soil venting with the venting pressure of 0.5 atm. In contrast, soil types with low relative permeability show minimal change, maintaining residual CH<sub>4</sub> concentrations above 500 ppm at the end of soil venting. Furthermore, as the venting pressure increases from 0 atm to 0.5 atm, the residual gas concentration at the bottom of venting bar hole significantly decreases, especially in the high soil permeability condition ( $k=2.9\times 10^{-11} \text{ m}^2$ ), within 60 minutes of soil venting. However, in the low soil permeability condition ( $k=5\times 10^{-12} \text{ m}^2$ ), the concentration remains elevated above appropriate residuals. These results indicate that the efficiency of soil venting is significantly impacted by the soil permeability as well as operating pressures. Thus, the soil properties should be considered in the site investigation in the soil venting at the field.

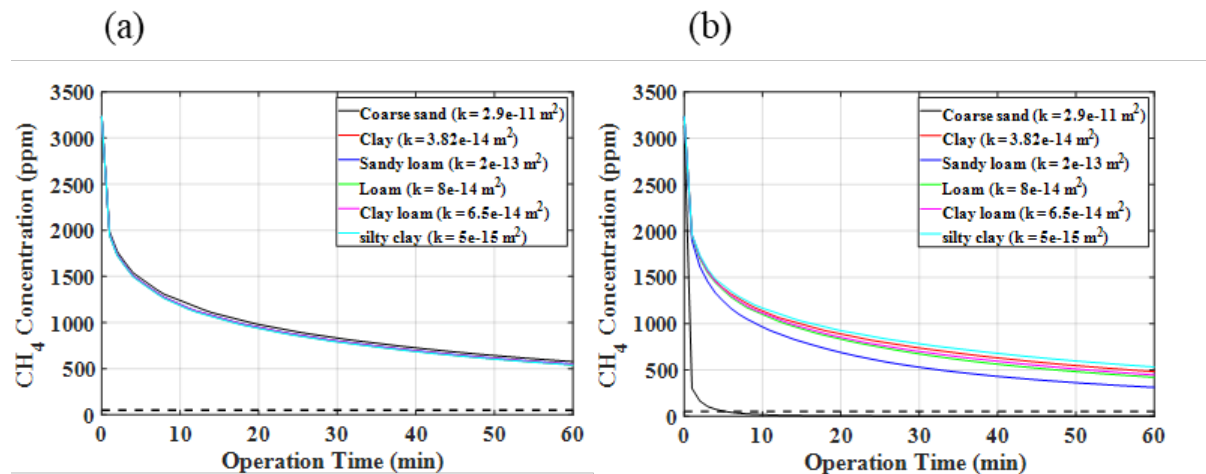


Figure 5: The change in the residual CH<sub>4</sub> concentration at the bottom of the venting bar hole during one hour of soil venting under venting pressures of (a) 0 atm, (c) 0.2 atm, and (e) 0.5 atm, respectively. The surface pressure in the model was given as the gauge pressure of 0 atm.

Figure 6 describes the change in the radius of influence with venting pressures of 0, 0.2, and 0.5 atm in six soil scenarios. The radius of influence is the radius extending from the barhole location to the distance the barhole can influence when a vacuum is applied to remove the gas from the soil. As the venting pressure increases from 0 to 0.5 atm, the radius of influence also increases. This expansion indicates that higher venting pressure enhances the advective gas flow through the soil, extending the effective soil venting area. However, the radius of influence does not



significantly change with variations in soil permeability in the current simulations. The reason might be that the proposed venting pressure in the model does not meet the air entry pressure of the soil, which is the pressure that can drive the movement of airflow in the soil pores. Therefore, soil properties might be a crucial factor considered in the operation of soil venting to determine an appropriate venting pressure.

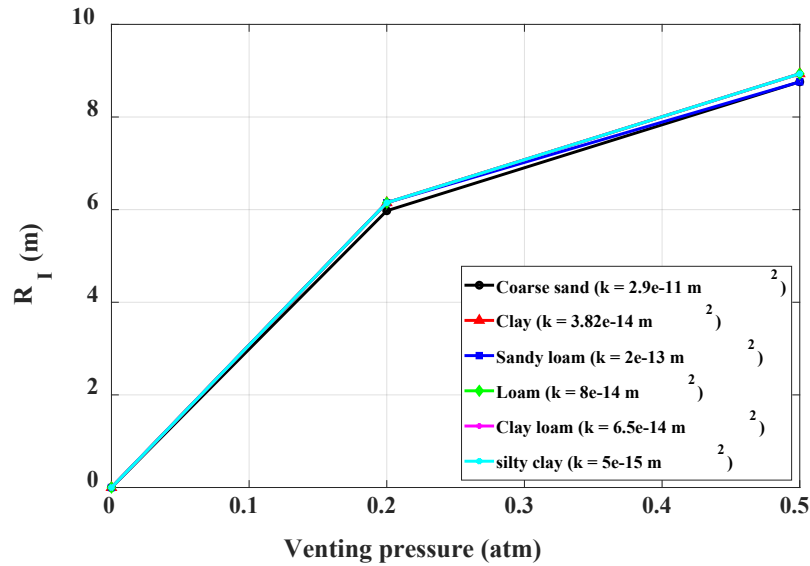


Figure 6: The radius of influences in six soil conditions with the venting pressure from 0 atm to 0.5 atm in the scenarios with a venting bar and three venting bar holes.

The estimated venting flow rates, based on the estimated radius of influence with varying soil permeability and the number of bar holes, are presented in Figure 7. As the venting pressure increases, the venting flow rate, or amount of gas removed over time, also increases. With a venting pressure of 0.5 atm, the venting flow rate increases from  $2.04 \times 10^{-5} \text{ m}^3/\text{s}$  to  $1.12 \times 10^{-1} \text{ m}^3/\text{s}$  with an increase in soil permeability from  $5 \times 10^{-15} \text{ m}^2$  to  $2.9 \times 10^{-11} \text{ m}^2$ . As the number of venting bar holes increases from one (1BH) to three (3 BH), the venting flow rate is higher than that of a single venting bar hole. Additionally, the venting flow rate from a venting bar hole with a venting pressure of 0.5 atm is higher than the venting flow rate from three venting bar holes with a venting pressure of 0.2 atm. This result suggests that the impact of venting pressure and the number of venting bar holes is important. Knowledge of this relationship can help to achieve cleanup goals and timelines. Further details on Soil Venting Systems can be found under Appendix 4.



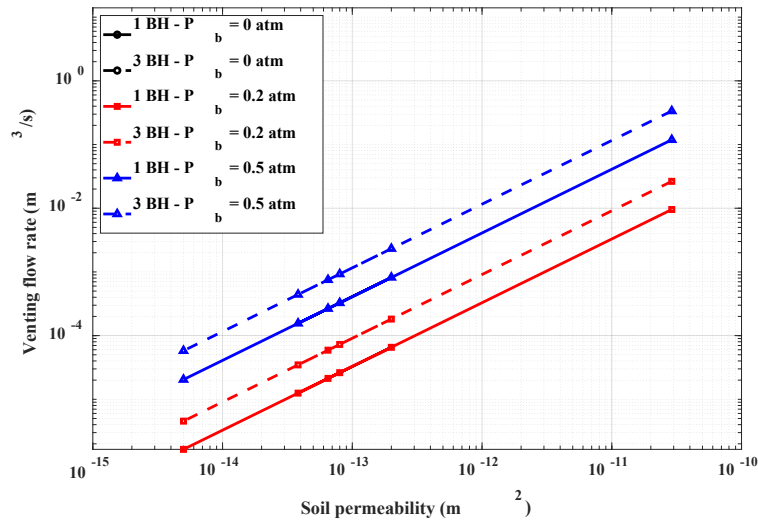


Figure 7: The variation of venting flow rates in six soil permeability scenarios based on one venting bar hole (1 BH) and three venting bar hole (3BH) scenarios. The red and blue lines present the venting flow rate with the venting pressure of 0.2 atm and 0.5 atm, respectively. The solid line indicates the scenario with a venting bar hole (1 BH). The dashed line describes the scenario with three venting bar holes (3 BH)

## 5.5 Key Findings

- The efficacy of soil venting is significantly impacted by the soil permeability. For the scenarios tested, with the same soil venting pressure (0.5 atm), the gas concentration decreases by 99% in highly permeable soil such as sand while only decreasing by 85% for a low permeable soil such as loam or clay, over the same one-hour period. This is further complicated by elevated soil moisture saturations which decrease the soil permeability. To achieve concentrations less than the 50-ppm level required for site cleanup, for most soil conditions, clean up times longer than 1 hr are required. Knowledge of the soil type and some general understanding of the soil moisture saturation can help guide the understanding of the removal times.
- The venting pressure is a sensitive parameter affecting the extent of the bar hole's radius of influence and therefore the effective soil venting area and required number of bar holes to achieve clean up goals. Knowledge of soil permeability, based on the soil type and moisture condition can help guide the selection of the appropriate pressures and number of bar holes needed.

- Comparison between the venting flow rates, number of venting bar holes, and venting pressure indicates that the venting pressure is more sensitive than number of venting bar holes to the development of venting flow rates in the soil venting system.

## **6. Deliverables 7, 8, 9, 12, and 14: Comprehensive data sets and understanding of the degree to which parameters affect the subsurface natural gas migration with significant flow rates**

### **6.1 Objective**

Analyze and compile the experimental data sets for follow on analysis.

### **6.2 Activities**

The experimental results from the 150 experiments were analyzed and reported in (1) this final report (2) peer reviewed publications and (3) publicly available data sets on the Texas Data Repository (TDR) (<https://dataverse.tdl.org/>) and Dryad Data Repository (<https://datadryad.org/stash>). Data can be accessed via the links given below.

1. Jayarathne, J.R.R.N.; Kolodziej, R.S.; Riddick, Stuart N; Zimmerle, D.J.; Smits, Kathleen M, 2023, "Replication Data for: Flow and Transport of Methane from Leaking Underground Pipelines: Effects of Soil Surface Conditions and Implications for Natural Gas Leak Classification", <https://doi.org/10.18738/T8/MQ5AQR>, Texas Data Repository, V1.
2. Mbuu, Mercy et al. (2023). Data from: Using controlled subsurface releases to investigate the effect of leak variation on above-ground natural gas detection [Dataset]. Dryad. <https://doi.org/10.5061/dryad.ncjsxkt15>
3. The data sets for this study are found in the reference: Fancy Cheptonui; Riddick N. Stuart; Anna Hodshire; Mercy Mbuu; Kathleen M. Smits; Daniel J. Zimmerle; Replication Data for Estimating the below-ground leak rate of a Natural Gas pipeline using above-ground downwind measurements: THE ESCAPE<sup>-1</sup> MODEL, [https://datadryad.org/stash/share/hrNNi7QftejUvLLT2Nahi2tM26ilVLk36\\_Qe8NYA\\_ToM](https://datadryad.org/stash/share/hrNNi7QftejUvLLT2Nahi2tM26ilVLk36_Qe8NYA_ToM) (accessed on 6 September 2023), Dryad data repository.

4. Tian, Shanru; Smits, Kathleen M.; Cho, Younki; Riddick, Stuart; Zimmerle, Daniel; Duggan, Aidan. 2022. Replication data for estimating methane emissions from underground natural gas pipelines using an atmospheric dispersion-based method, <https://doi.org/10.18738/T8/UAO5XX>, Texas Data Repository, V1.
5. Cho, Younki; Smits, Kathleen M.; Steadman, Nathaniel L.; Ulrich, Bridget A.; Bell, Clay S.; Zimmerle, Daniel J., 2022, “Replication Data for: A Closer Look at Underground Natural Gas Pipeline Leaks Across the United States”, <https://doi.org/10.18738/T8/32VPN0>, Texas Data Repository, V1

### 6.3 Summary of Experiments Conducted

Overall, 150 field experiments were completed during a period of 24 months (August 2021 – August 2023). The experiments measured the unsteady state during the leak, the steady state during the leak, and the unsteady state measurements after terminating the leak as shown in Table 3 below. More details can be found in Appendix 5.

*Table 3: Summary of the experiments conducted to collect data sets including the experiment dates, parameter considered, leak depth, leak rate, gas composition, surface-subsurface condition, and water saturation.*

Parameter	Exp #	Date started (dd/mm/yy)	Leak rate (slpm)	Release period (hrs)	Gas composition	Surface cover	Belowground infrastructure	Water saturation (%)
Leak rate	1 a,b,c	11/11/21	10	24	Dry	Grass	none	25
	2 a,b,c	11/11/21	10	24	Dry	Grass	none	25
	3 a,b,c	03/12/21	35	24	Dry	Grass	none	25
	4 a,b,c	01/12/21	35	24	Dry	Asphalt	Pipe	25
	5 a,b,c	15/11/21	50	24	Dry	Grass	none	25
	6 a,b,c	19/11/21	50	24	Dry	Asphalt	Pipe	25
Moisture	7 a,b,c	25/03/22	10	24	Dry	Moisture cap	none	40

	8 a,b,c	23/03/22	10	24	Dry	Asphalt+ moisture cap	Pipe	40
	9 a,b,c	05/04/22	35	24	Dry	Moisture cap	none	40
	10 a,b,c	30/03/22	35	24	Dry	Asphalt+ moisture cap	Pipe	40
Snow cover	11 a,b,c	17/02/22	10	24	Dry	Snow	none	25
	12 a,b,c	23/02/22	10	24	Dry	Snow	none	25
	13 a,b,c	02/03/22	10	72	Dry	Slush	none	25
	14 a,b,c	07/03/22	10	72	Dry	Slush	none	25
Slush	15 a,b,c	08/12/21	10	24	Dry	Frost	none	25
	16 a,b,c	13/12/21	35	24	Dry	Frost	none	25
Surface cover	17 a,b,c	30/06/22	10	24	Dry	Semi	none	25
	18 a,b,c	26/07/22	10	24	Dry	Semi	none	25
Subsurface complexity	19 a,b,c	21/04/22	10	24	Dry	Asphalt	Open Pipe	25
	20 a,b,c	11/04/22	35	24	Dry	Asphalt	Open Pipe	25
Soil Moisture	21 a,b,c	02/05/22	10	24	Dry	Moisture cap	none	40
	22 a,b,c	04/05/22	10	24	Dry	Asphalt+ moisture cap	Pipe	40
Surface cover	23 a,b,c	13/07/22	10	24	Dry	Full	none	25
	24 a,b,c	19/07/22	10	24	Dry	Full	none	25
Leak rate	25 a,b,c	20/06/22	100	6	Dry	Grass	none	25
	26 a,b,c	28/06/22	200	6	Dry	Grass	none	25
	27 a,b,c	07/07/22	100	6	Dry	Grass	none	40
Gas compositi	28 a,b,c	19/07/22	10	24	Wet	Grass	none	25
	29 a,b,c	02/08/22	10	24	Wet	Grass	none	25

	30 a,b,c	29/08/22	10	24	Dry	Grass	none	25
Surface condition	31 a,b,c	14/06/23	10	120	Dry	Grass	none	25
	32 a,b,c	21/06/23	10	120	Dry	Grass	none	25
	33 a,b,c	31/07/23	10	120	Dry	Moisture cap	none	40
a – Unsteady state measurements during the leak b – Steady state measurements c – Unsteady state measurements after terminating the leak Moisture cap – A saturated layer of near surface soil (4 inch downwards from the soil surface)								

## 6.4 Effect of Leak Rate

Figure 8 compares two groups of leak rates drawn from the experiments in Table 3. All experiments had the same surface cover – grass – and similar soil moisture. The first three experiments had relatively low leak rates of 10, 35, and 50 slpm (21, 74, and 105 scfh), while the last two experiments had high leak rates of 100 and 200 slpm (212 and 424 scfh). The Figure 8 shows the belowground CH<sub>4</sub> plume patterns 6 hours after leak initiation to show the critical period when outward gas migration is fastest, and 24 hours after leak termination to illustrate behavior after first responders intervene and terminate the leak.

The three smaller leaks show a similar, bulb-shaped gas concentration profile at 6 hours, indicating similar concentrations at the first row of measurement points. Experimental data indicate the volume with gas concentrations near 100% (i.e. other gases have been fully displaced) falls within the first measurement points. For leak rates of 100 slpm and 200 slpm (212 and 474 scfh), the belowground CH<sub>4</sub> plume edge at 6 hours expanded 2.8 m (9 ft) from the leak point, a 2.3-times increase in plume width (approximately 5-times increase in underground volume) compared to the 10 slpm (20 scfh) case, indicated by high concentrations at the first row of measurement locations. Additionally, the underground volume where gas concentrations are near 100% expanded substantially (to first row of sensors), indicating a larger underground volume storing a high gas concentration.

In all five cases, the edge of the measured concentrations is similarly sharp, indicating that advective transport dominates – predominately vertical in the smaller three cases, both vertical and

horizontal in the larger two cases. Therefore, higher leak rates resulted in faster, and initially further, gas migrations for the high concentrations; but given this surface cover of grass, transport near the leak has influence on concentrations further from the leak location.

When the leak was terminated, the three lower leak rates return to background concentrations within 24 hours – there is sufficient transport from the surface to fully clear the leak. The two larger leaks, however, ‘stored’ more gas in the subsurface, and 24 hours is insufficient to clear the leak.

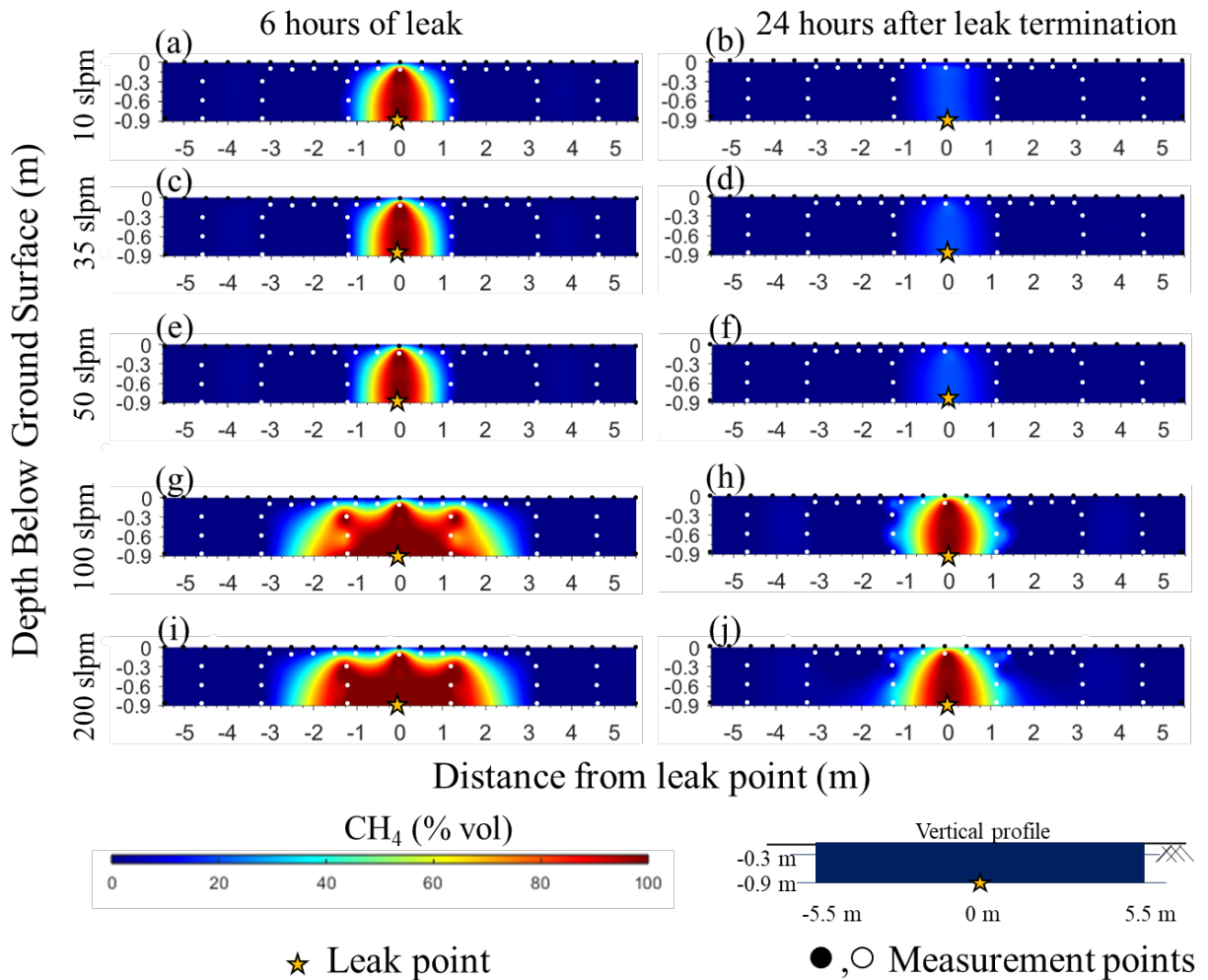


Figure 8: Subsurface methane concentration distribution at 6 hours after leak initiation and 24 hours after leak termination experiments with leak rates 10, 35, 50, 100, and 200 slpm. (a), (c), (e), (g), (i) are vertical profiles for 6 hours after leak initiation, and (b), (d), (f), (h), (j) are vertical profiles 24 hours after leak termination. The respective belowground profile key for each experiment, the location of the leak point, and measurement points are also shown. Surface and subsurface measurement points are shown in black and white dots respectively. Profiles are created considering a homogeneous soil structure along all directions.

## 6.5 Effect of Surface Condition

Effects of surface covers were compared using Experiments 12 through 14, 17,18, 23, and 24. Selected experiments for the comparison include Grass-Dry (baseline case), Asphalt-Dry, Grass-Moist, Asphalt-Moist, Grass-Snow, and Asphalt-Snow surface conditions. This section is also available as Deliverable 17: Jayarathne et al. (2024).

Figure 9 shows the subsurface CH<sub>4</sub> distributions at 6 and 24 hours after the 10 slpm (20 scfh) leak was initiated and 24 hours after the leak was terminated. Comparing wet to dry conditions for the grass surface cover, the area of high gas concentration at the surface for wet is much smaller than the underlying gas migration belowground, due to the soil moisture in the topsoil layer (panels (g) and (h)). The Grass-Snow scenario was not measured at the surface but illustrates a similar spreading of the belowground plume. Comparing these two panels to the Asphalt-Dry case indicates that moisture has transformed the gas spreading behavior of the grass-covered leak into one that more closely resembles the same leak under an asphalt surface. The spreading of gas leaks under paved areas is a hazard well known to operational personnel. These data indicate that sufficient moisture or snow to fill pores in the topsoil layer may transform the gas migration behavior of a vegetation-topped leak into that of a pavement-topped leak location.



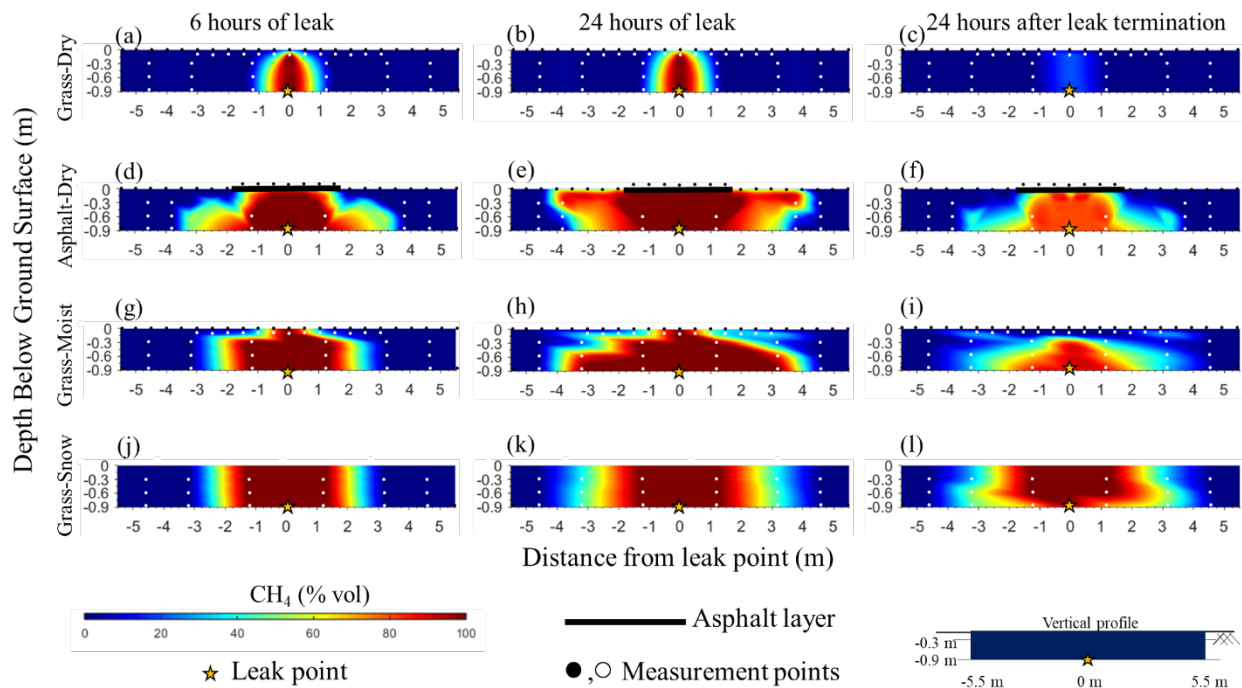


Figure 9: Subsurface methane concentration distribution at 6 and 24 hours after leak initiation and 24 hours after leak termination for Grass-Dry, Asphalt-Dry, Grass-Moist, and Grass-Snow experiments. (a), (d), (g), (j), and (b), (e), (h), (k) are vertical profiles for 6 and 24 hours respectively after leak initiation. (c), (f), (i), (l) are vertical profiles for 24 hours after leak termination. The respective belowground profile key for each experiment, the location of the leak point, measurement points, and the asphalt layer are also shown. Surface and subsurface measurement points are shown in black and white dots respectively. Profiles are created considering a homogeneous soil structure along all directions.

These data have important implications for leak detection, grading, and response. First, when grading leaks, a vegetation-covered area should be evaluated as if it were covered by an impermeable or semi-permeable layer. Second, during a leak response in wet weather, first responders should anticipate that the observed surface extent of a leak may deviate substantially from the underground gas plume.

In addition to a wider extent of gas migration, the speed of migration was also accelerated when surface permeability reduced due to moisture or snow. Under Grass-Dry conditions, the belowground plume reached its maximum width of 4 feet within 2.5 hours. For the same leak rate in Asphalt-Dry, the belowground plume expanded 3 times farther than the Grass-Dry plume and took 7 times longer to reach this maximum width. This indicates that the Grass-Dry case was in equilibrium with the atmosphere within 2.5 hours, such that the gas from the leak was balanced by

gas lost to atmosphere. The asphalt condition took 7 times as long to achieve the same equilibrium condition and creating a much larger quantity of gas underground. Therefore, the presence of the impermeable cap increased the surface area of the leak expression (high concentration area at the surface), even though the same amount of gas was being transported to the surface.

It is also important to note that in the asphalt case, the width of the gas plume at the sides of the pavement is larger than the underground extent of gas migration. This is the reverse of a leak with a vegetation cover in moist conditions. For moist conditions, the area of high surface concentration is *smaller* than the underground plume, while for dry conditions with an impermeable cover, the high surface concentrations *extend farther* than the underground plume. First responders should note that, while the moisture causes gas to migrate underground *as if* there were an impermeable cover, surface readings will not behave the same as a fixed impermeable cover (e.g. pavement, asphalt, concrete, etc.). In the Grass-Moist condition, a small surface expression will likely be seen and there will be few physical clues on the surface that the underground plume is much larger than the area of high concentration at the surface. In contrast, in the case of pavement, the size of the capping layer is visually evident, encouraging an estimate of minimum plume size.

Moisture also impacts gas retention time after the leak is terminated. For Grass-Dry, the leak clears in less than 24 hours. Clearing time increases by 5-7 times that of the dry conditions for moisture, snow, or asphalt conditions; the highest retention time (7 times) was under snow conditions. In these experiments, CH<sub>4</sub> trapped under snow, moist soil, and asphalt surface conditions persisted for up to 12 days with 5-15% CH<sub>4</sub> (v/v) conditions persisting underground up to 7.5 days.

In an emergency scenario where a gas leak has been discovered shortly after initiation, the gas may be actively moving outward due to advection, creating a pronounced concentration gradient between areas of high and low gas concentration. When the leak is terminated, this high gradient still exists, and gas will continue to move via diffusion. This movement extended the outermost boundary of the plume by about 2-4% for each case.

Finally, the surface condition impacts the speed of gas migration underground, and that speed is not uniform through the soil profile but rather dependent on the concentration contour (e.g. 0.1% or 5% v/v), see Figure 10. We focus on the 5 and 15% CH<sub>4</sub> (v/v) contours. For these high concentration contours, the gas migration rates for the asphalt, snow, and wet-soil surface

conditions were generally 3.5 times faster than the dry grass conditions. As a result, this creates a much larger zone with high gas concentrations than the dry base case conditions. Specifically, in the same amount of time as the dry conditions, the asphalt, wet, and snow conditions result in a high concentration zone 3-7 times larger than the grass dry base case.

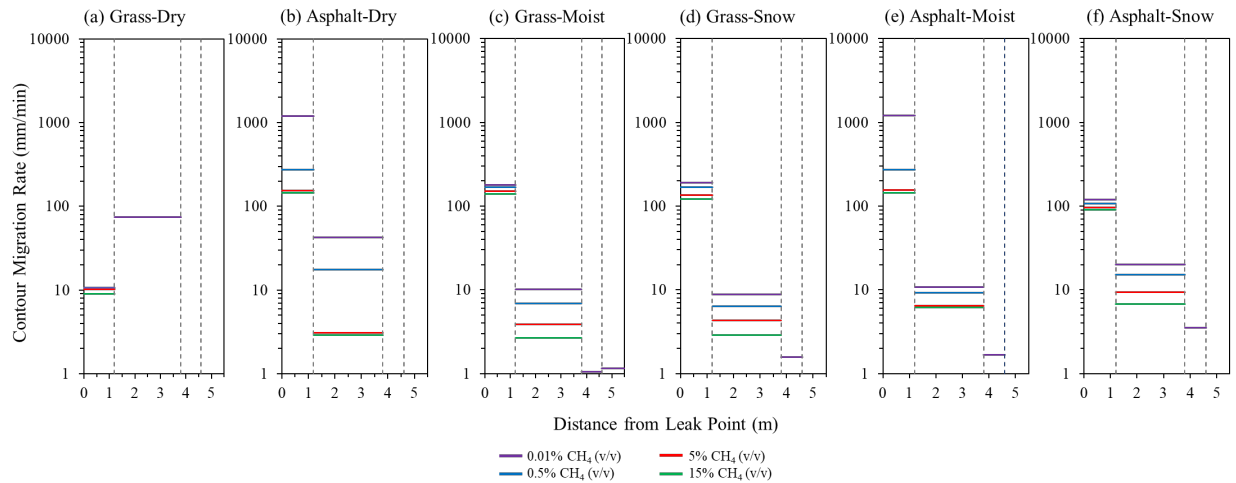


Figure 10: Variation in migration rate for 0.01%, 0.5%, 5%, and 15% CH<sub>4</sub> (v/v) contours under (a) Grass-Dry, (b) Asphalt-Dry, (c) Grass-Moist, (d) Grass-Snow surface conditions. The distances between each measurement point are represented by dotted vertical lines at 1.2, 3.2, and 4.6 m along the x-axis.

In summary, adding a capping moisture layer to a vegetation-covered leak will produce underground gas migration resembling that of pavement in migration speed and size. However, concentrations measured at surface *will provide no indication* of the increased gas migration extent. Therefore, in wet conditions, first responders are encouraged to treat leaks in vegetative areas *as if they were covered by pavement*, and to not expect high surface concentrations to accurately represent the size of the plume. In these cases, bar hole surveys below the wet topsoil layer may provide a better assessment of gas migration extent.

## 6.6 Effect of Gas Composition

The effect of gas composition was compared using experiments 28 through 30. Results show that increase of ethane and propane composition of the mixture (wet gases) results in greater migration of high concentration contours (represented by LEL and UEL concentrations) compared to dry gas. In contrast, lower concentration contours (10% of LEL) did not show any variation in

migration distance. However, migration rates were decreased by orders of 1/10 for wet gases compared to dry gas.

Shown in Figure 11 below are the variation of explosive limit durations and travel distances as the composition of gas changed under a leak rate of 10 slpm (20 scfh). Methane, which is lighter than normal air (density = 0.55 kg/m<sup>3</sup> at STP), was mixed with other hydrocarbons, ethane (density = 1.28 kg/m<sup>3</sup>) and propane (density = 1.88 kg/m<sup>3</sup>), which are heavier than normal air. In addition to density, changing gas mix also impacts the diffusion coefficients of the gas (diffusion coefficients for methane, ethane, and propane in air are 0.221 cm<sup>2</sup>s<sup>-1</sup>, 0.128 cm<sup>2</sup>s<sup>-1</sup>, and 0.10 cm<sup>2</sup>s<sup>-1</sup> respectively).

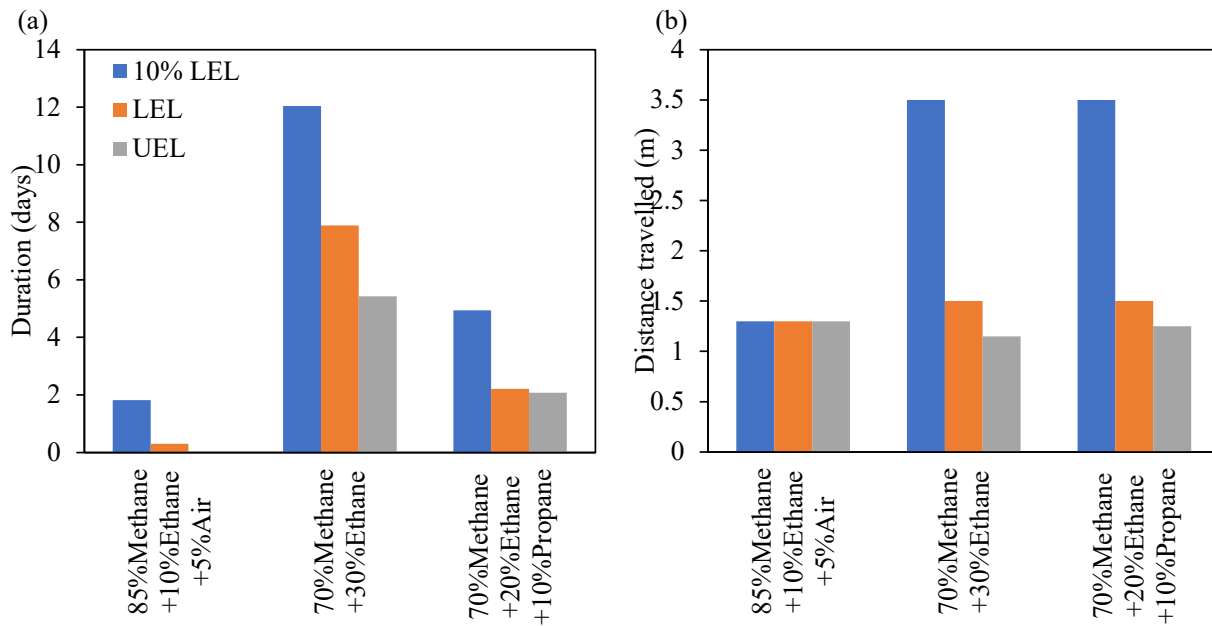


Figure 11: Variation in flammable limits (10%LEL=0.5% CH<sub>4</sub>(v/v), LEL = 5% CH<sub>4</sub>(v/v), and UEL=15% CH<sub>4</sub>(v/v)) (a) duration and (b) travel distance for 20 scfh (10 slpm) leaks under different gas compositions of methane, ethane, propane, and air.

Adding ethane and propane to the gas mixture increases the density of the mixture relative to the base case gas (85% of methane, 10% ethane, and 5% air) and the diffusion coefficient has decreased. This combination of changes tends to increase gas retention within the soil structure and reduces upward migration and emission through the soil-air interface. Relative to dry, market-grade gas, the 10% LEL duration has increased by a factor of 6 and LEL by a factor of 26. The

UEL contour, which was limited to <1 hr for distribution gas, persisted for 5.5 days by adding 30% ethane to the gas mixture.

## **6.7 Effect of Combined Surface Subsurface Anomalies**

Figure 12 shows the 2D distribution of belowground CH<sub>4</sub> concentrations 6 and 24 hours after the leak initiation and 24 hours after leak termination for selected subsurface anomalies. The subsurface conditions considered are:

- Unpaved undisturbed dry soil (baseline case)
- a trench with backfilled soil a buried pipe under an asphalt pavement (trench with pipe)
- trench with partially saturated soil under an asphalt pavement (trench with moist soil)
- trench with partially saturated backfilled soil with a buried pipe under an asphalt pavement (trench with moist soil and pipe).

As discussed before, the CH<sub>4</sub> plume under undisturbed dry soil conditions (i.e. the baseline case) forms a bulb-shaped plume with a maximum width of 1.2 m for a leak 0.9 m (3 ft) deep. The belowground plume stabilized within 6 hours after initiating the leak, and as a result, the plume shape and width did not change between 6 and 24 hours after leak initiation. When the surface complexity increased to a trench with disturbed soil under an asphalt pavement (trench with pipe), CH<sub>4</sub> plume width increased to 3.8 m at 0.9 m (3 ft) belowground and remained at that width between 6 and 24 hours. Although an increased plume width was observed at 0.9 m (3 ft) depth, CH<sub>4</sub> plume at the near-surface layer is more diffused and a vertical concentration gradient could be seen. However, the increase in air-pore connectivity and the respective diffusivity not only increased the lateral migrations but also increased the atmospheric dilution across the soil-air interface. A wider, diluted, plume can be attributed to the simultaneous lateral and vertical diffusions.

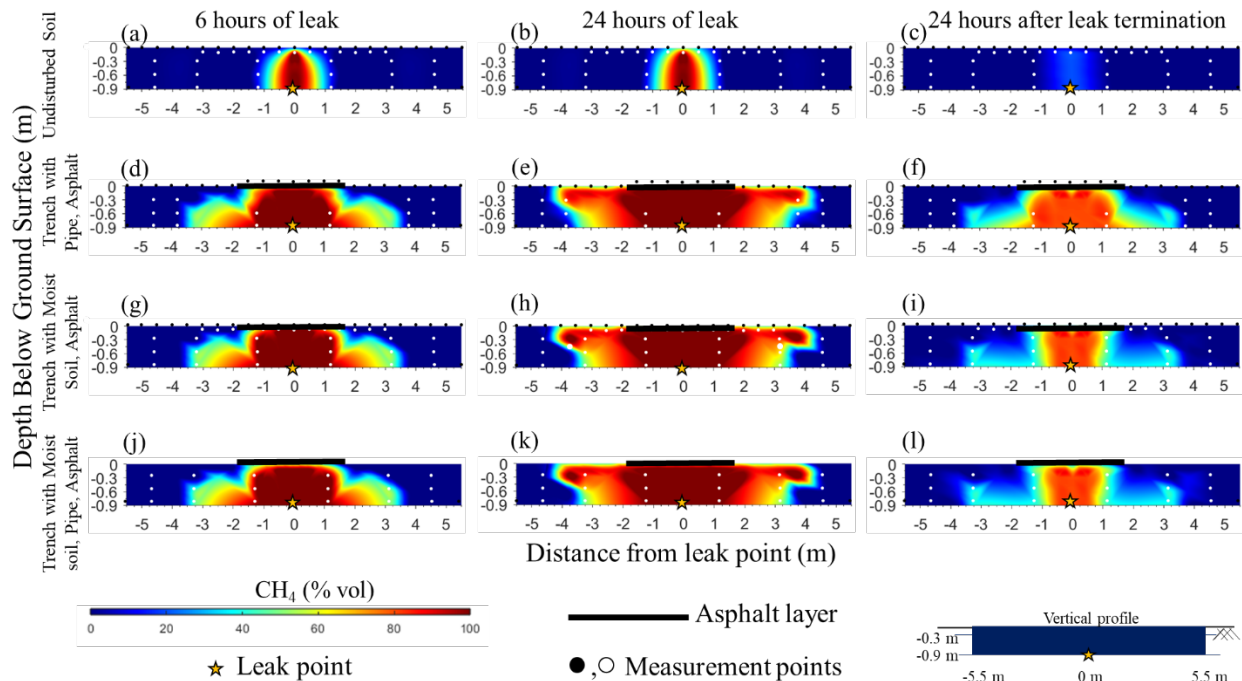


Figure 12: Subsurface methane concentration distribution at 6 and 24 hours after leak initiation and 24 hours after leak termination for Undisturbed Soil under Asphalt pavement, Trench with Pipe under Asphalt pavement, Trench with Moist Soil under Asphalt pavement, and Trench with Pipe Moist soil and Pipe under Asphalt pavement experiments. (a), (d), (g), (j), and (b), (e), (h), (k) are vertical profiles for 6 and 24 hours respectively after leak initiation. (c), (f), (i), (l) are vertical profiles for 24 hours after leak termination. The respective belowground profile key for each experiment, the location of the leak point, measurement points, and the asphalt layer are also shown. Surface and subsurface measurement points are shown in black and white dots respectively. Profiles are created considering a homogeneous soil structure along all directions

Detailed descriptions on belowground CH<sub>4</sub> plume behavior are given under Appendix 5 and 6. After determining the migration extent, resulting plume pattern, concentration variation during the leak period, as well as after terminating the leak under different experimental parameters given in Table 3; NG migration patterns were then used to determine the variation in potential hazards.

## 6.8 Belowground Flammable Threat zone and Methane Contaminated Zone

**Error! Reference source not found.** shows the belowground migration rate of 15%, 5%, 0.5%, and 0.01% CH<sub>4</sub> (v/v) contours. While the belowground concentration profiles are unique to each surface condition, the migration distances varied based on the concentration profile of interest. Grass-Dry had the slowest belowground migration rates and Asphalt-Dry the largest.

Grass-Snow and Grass-Moist conditions were close seconds (**Error! Reference source not found.a-d**). Based on the belowground locations of the 15% and 5% CH<sub>4</sub> (v/v) contours, the belowground “Flammable threat zone”, defined as the area with potential flammability, was determined. Based on the belowground location of the 0.01% CH<sub>4</sub> (v/v) contour, the belowground “CH<sub>4</sub> contaminated zone”, defined as an area subjected to CH<sub>4</sub> contamination, was determined (**Error! Reference source not found.e, f**). Here, we compare the active leak period and after leak termination. Gas migration rates under Asphalt-Dry (0.01% contour) were 3.5 times farther than Grass-Dry. This increased the belowground CH<sub>4</sub> contaminated area by a factor of 12.5 relative to Grass-Dry. The ~3.4 times faster 5% and 15% contours created a ~7 times larger flammable threat zone, ~3 times farther from the leak point, compared to the Grass-Dry conditions. For Grass-Moist, 3.5 times faster migration of 5% and 15% contours created a ~4.5 times larger flammable threat zone, ~2.6 times farther from the leak point compared to the Grass-Dry condition. The 0.01% CH<sub>4</sub> (v/v) contour migration distance increased up to 4.5 times as the Grass-Dry, resulting in 12 times larger CH<sub>4</sub> contaminated zone. Continued lateral migration of 15% and 5% CH<sub>4</sub> (v/v) contours under Grass-Snow resulted in a ~5.5 times larger and 1.4 times shifted flammable threat zone compared to Grass-Dry.

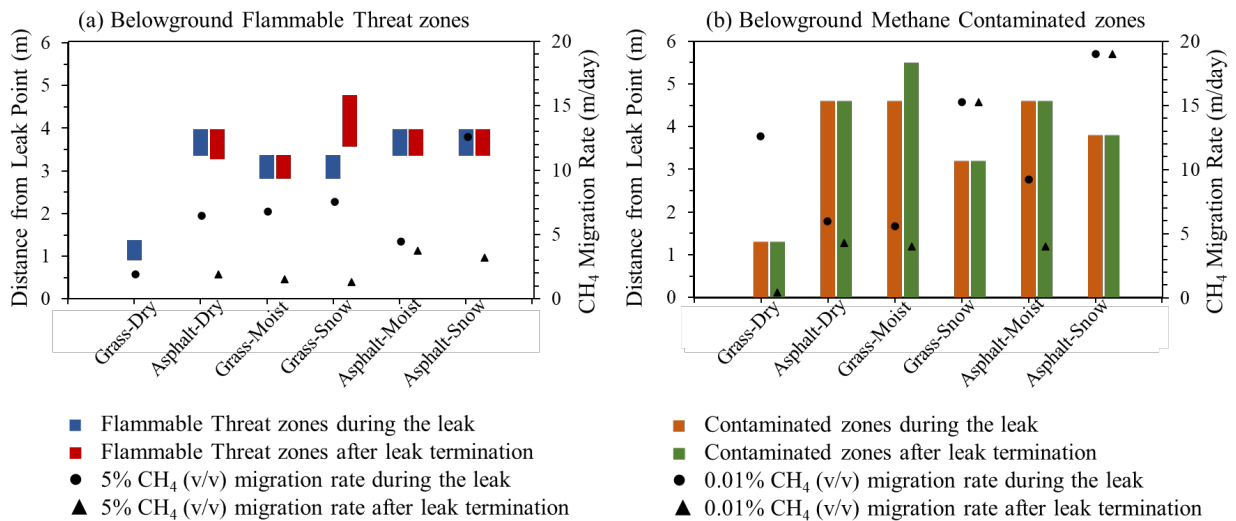


Figure 13: Variations in (a) Belowground flammable threat zones based the on belowground location of the 5% and 15% CH<sub>4</sub> (v/v) contours and (b) Belowground methane-contaminated zone based on the belowground location of 0.01% CH<sub>4</sub> (v/v) contours. The overall migration rates are also shown. Here the location and migration rates are shown for both the active leak period and after leak termination.

Common to all surface conditions, the migration rate of the 15% CH<sub>4</sub> (v/v) contours are similar within each respective measurement interval (i.e., between measurement points). In contrast, a large variation in migration rates can be seen among other contours of interest, distinguishing between each surface condition. Asphalt-Dry showed the largest lateral migration rates with magnitudes spanning over a large range among different concentration contours. This implies that the plume migrates faster but with a smooth edge of gradually decreasing contours. Grass-Moist and Grass-Snow showed narrow ranges in migration rate magnitudes among different contours defining a sharp plume edge. Both conditions have sparsely disturbed concentration profiles limiting the space between the plume boundary and the higher concentration profile. The observations show that the nature of the surface cover can define the nature of the plume edge to be smoothly expanding over a large area versus a sharp edge.

## **6.9 Surface Expression of Belowground NG Plumes**

Figure 14 shows the belowground vertical and horizontal profiles for a 10 slpm (20 scfh) belowground leak under unpaved, undisturbed, dry loam soil conditions after 6 hours of gas leakage. The vertical profile shows a bulb-shaped distribution, centered on the leak point. The vertical profile allows one to visualize the narrow plume width at the surface level compared to the wider profile at the depth of the leak point, and substantial gas migration below the leak depth. As methane is a light gas compared to air, it has the tendency to preferentially move upwards due to buoyancy. However, lateral and downward movement also occur due to diffusion (Figure 14a). Horizontal profiles (Figure 14 b– e) show the plume extents at four different depths, obtained using a CGI (at the surface) and CH<sub>4</sub> concentration sensors at lower depths. Our observations show that under dry soil conditions, the width of the plume 0.9 m (3 ft) belowground is 4 times wider than the plume observed at the surface. In other words, gas may have migrated much further below ground than is represented by the surface expression of the leak.



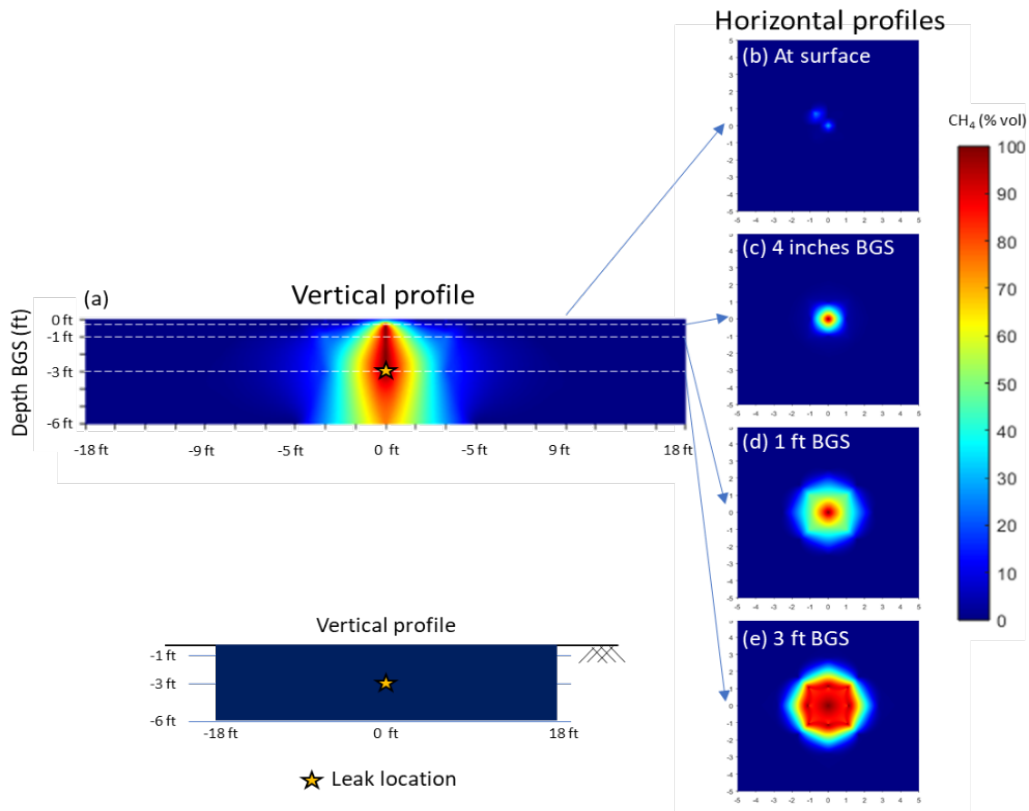


Figure 14: Belowground Vertical and horizontal  $CH_4$  profiles for a 10 slpm NG leak under unpaved undisturbed dry soil conditions.

Figure 15 shows the belowground vertical and horizontal profiles for a 10 slpm (20 scfh) belowground leak under unpaved, undisturbed, moist loam soil after a heavy rain event after 24 hours. Unlike the dry conditions, the upward bulb-shaped contours were not visible. Rather, due to the influence of the elevated near-surface soil moisture, the gas expanded laterally immediately below the surface, relative to the dry soil condition. When the ground is wet, surface concentrations measured using a CGI further decreased making the plume practically invisible from the surface (Figure 15b), while relatively wide gas migration was observed 0.1 m (4 in) deep – migration in excess of the widest profile in dry soil conditions. The observed plume width is 16-times wider than the detected surface plume and 7-times wider than the plume observed under dry soil conditions. Therefore, under wet soil conditions, negligible surface methane concentrations are not indicative of the gas accumulation below the surface, even at shallow depths. Similar conditions were seen in all moisture experiments performed in this study: heavy rain (shown in

Figure 15), ice/snow, and light rain. Insufficient experiments were performed to identify when gas migration transitions from the ‘dry’ behavior to the ‘wet’ behavior; further work in this area is recommended.

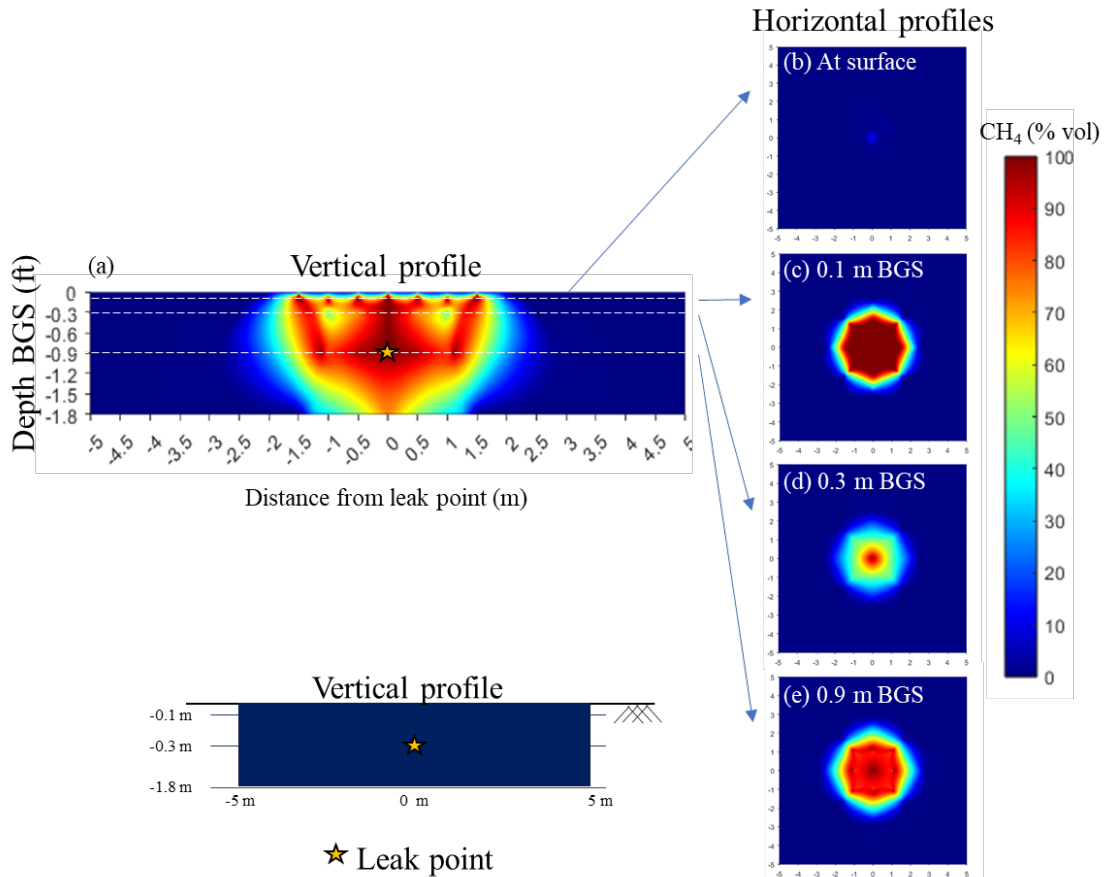


Figure 15: Belowground Vertical and horizontal CH<sub>4</sub> profiles for a 10 slpm NG leak under undisturbed near surface moist soil conditions.

## 6.10 Key Findings

- **Leak rate:** An increase in leak rate [10 to 200 slpm (21 to 424 scfh)] increases NG accumulation around the leak location than lateral migrations. Although the increase in the leak rate through mid-range [2.2 – 35 slpm (4.4 – 70 scfh)] is proportional, the large leak [ $> 35$  slpm (70 scfh)] migration extent is not proportional to the leak rate. Although large concentrations move faster and farther during initial hours after a large leak starts,

small gas concentrations move slowly and far from the leak location at a similar rate for both small and large leaks.

- **Soil moisture:** An increase in soil moisture saturation influences in two ways. (1) If the moisture remains near the surface creating a moist topsoil layer (i.e., moisture cap), a small surface expression is detectable at the ground surface using typical methods, while gas accumulates immediately below the surface and at depth, creating relatively large lateral expansions. (2) If the moisture percolates further down to leak depth, lateral migration of the gas is reduced while vertical migration of the gas is increased (especially under significant leak rates).
- **Surface cover:** A belowground NG plume up to 3 to 4 times wider than the plume under uncovered, dry soil should be expected when the NG leak is under surface cover with poor permeability, such as asphalt, concrete, or wet surface conditions (snow or moist soil layers). Gas will also migrate horizontally faster than uncovered leak sites.
- **Gas composition:** Leaks from gathering lines should be treated differently than pipeline leaks from the transmission and distribution networks: Leaks in pipelines carrying heavier hydrocarbons (C2+) may travel up to three times farther and could remain in the ground six times longer. This suggests that set back distance for gathering lines should be larger, more caution is required to assure venting of gas from the soil, and repairs that require excavation should be delayed longer until gas has vented from the soil.
- **Soil structure:** Leaked gas migrates 3 times as far along trenches and cracks compared to undisturbed surrounding soil. Although not tested here, open conduits in the path of underground gas migration could produce even longer gas migration anomalies. First responder documents consider only trenches (or disturbed soil) as a cause for lateral gas migrations. However, lateral and downward migration of gas should be expected through both disturbed and undisturbed soils. Further, high concentrations along trenches and fractures may mask the actual leak location by creating high surface concentration some distance from the leak.

- **Leak Termination:** Terminating the gas leak does not remove the hazard from a leak site. Gas concentration of LEL and above exist for extended periods even after terminating with continued lateral migrations. While a leak site in uncovered, dry-soil conditions may clear in 24 hours, a site with reduced venting possibilities (i.e., surface conditions such as asphalt covers, snow covers, or wet soil layers) can take 7 days or more to clear. Therefore, the site should not be considered safe by terminating the leak; additional belowground monitoring should be completed.
- **Surface CH<sub>4</sub> concentrations:** In most cases, first responders should expect the size of the belowground gas plume to be larger than the gas detected using a CGI at the leak site ground surface. The expected belowground plume migration can extend to 4 or more times the size of the plume detected at the ground surface under dry, uncovered soil conditions. In general, more gas accumulation and larger lateral expansions should be expected under wet soil conditions than in the same location under dry conditions. Further, the detectable surface plume under wet conditions is likely to be smaller than the dry conditions for a given leak size, while the below ground plume is likely to be larger. While not experimentally tested in this work, a stable leak in dry conditions is likely to quickly transition to a wet condition pattern if soil moisture increases.
- **Soil temperature:** Changes in soil or air temperature do not make a significant difference to subsurface gas migrations.
- **Wind speed:** Increases in wind speed decreases the below ground concentrations of leaked natural gas.

## **7. Deliverable 13: Modeling tool to predict the behavior of underground leaks with significant flow rates**

### **7.1 Objective:**

To assist with experimental design and extend experimental results to additional diverse operating conditions, (e.g. additional soil types, surface covers, pipeline depths, leakage types etc.), numerical simulations are performed using computational models to guide observations and interpreted data. The model simulates two-phase (liquid and water) and two-component (CH<sub>4</sub> and air) transport in the vadose zone under isothermal conditions using COMSOL Multiphysics®. The models are first calibrated for transient behavior by matching experimental data for better performance.

### **7.2 Development and Optimization of Simulation Domain**

Figure 16 shows the simulation domain. Further details about the simulation domain, model formulations and related simulations can be found at Gao et al. (2021), Jayarathne et al. (2023), and Appendix 6: Understanding of the degree to which parameters affect the subsurface natural gas migration with significant flow rates: Simulation Report. Briefly, as seen in Figure 16, the simulation domain bottom was designed with a symmetric boundary, while the left and right sides of the domain were assigned with hydrostatic water pressure determined during ground saturation. The top boundary was given a flux top boundary condition to incorporate the atmospheric effect. Dry soil simulations were conducted with parameters matching field conditions (0 m<sup>3</sup>/m<sup>3</sup> initial methane volume fraction in soil, and 0.86 m<sup>3</sup>/m<sup>3</sup> of methane at the source. Initial bottom water saturations of disturbed soil = 0.2 m<sup>3</sup>/m<sup>3</sup>, undisturbed soil = 0.2 m<sup>3</sup>/m<sup>3</sup>, sand = 00 m<sup>3</sup>/m<sup>3</sup>, clay = 22 m<sup>3</sup>/m<sup>3</sup>, and initial top water saturations of disturbed soil = 0.125 m<sup>3</sup>/m<sup>3</sup>, undisturbed soil = 0.14 m<sup>3</sup>/m<sup>3</sup>, sand = 00 m<sup>3</sup>/m<sup>3</sup>, clay = 22 m<sup>3</sup>/m<sup>3</sup>). Simulation scenarios were selected to represent 1) leaks under different soil types, 2) leaks under soil-moisture saturations, 3) leaks under different surface conditions, 4) leaks associated with different subsurface anomalies, and 5) leaks associated with different surface and subsurface complexity combinates as shown in Table 2.

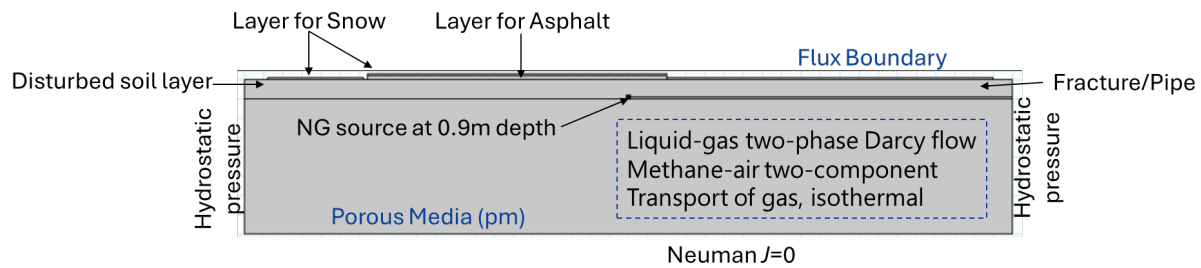


Figure 16: Integrated simulation domain representing soil matrix, leak point, surface and subsurface complexities, and boundary conditions.

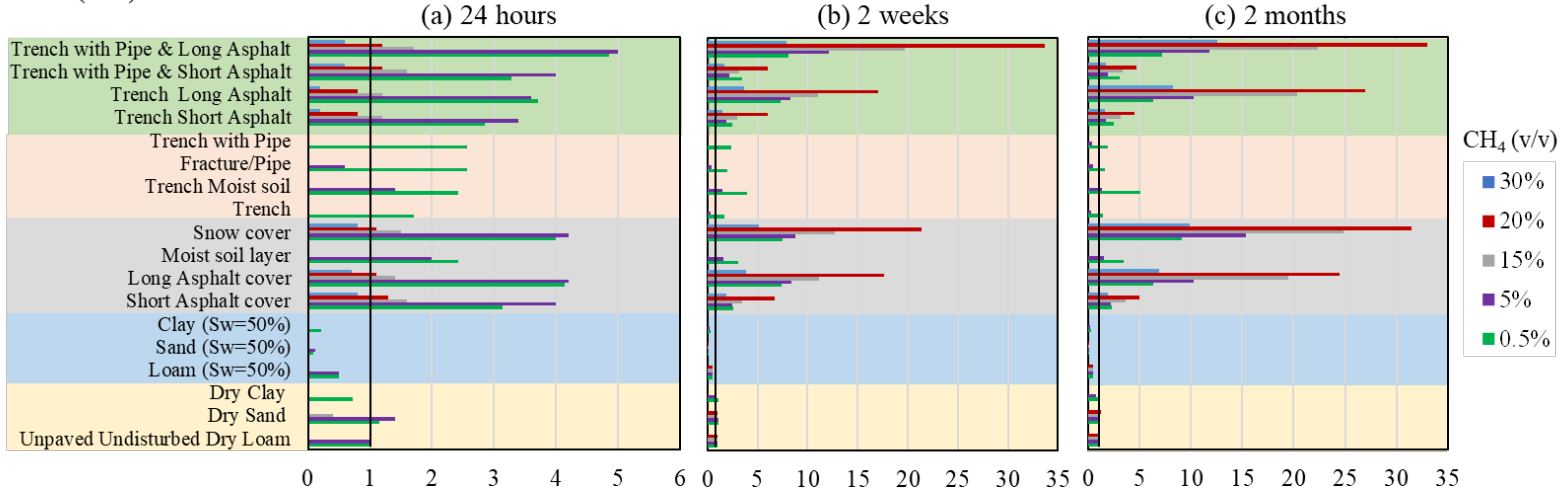
While detailed descriptions in subsurface CH<sub>4</sub> plume behaviors are described in Appendix 6, this section focuses on understanding the variation in migration rates, migration extents and long-term behavior of leaked NG in the subsurface. Simulation scenarios considered for the analysis are given in Table 2.

### 7.3 Variation in subsurface CH<sub>4</sub> migration extent and rate

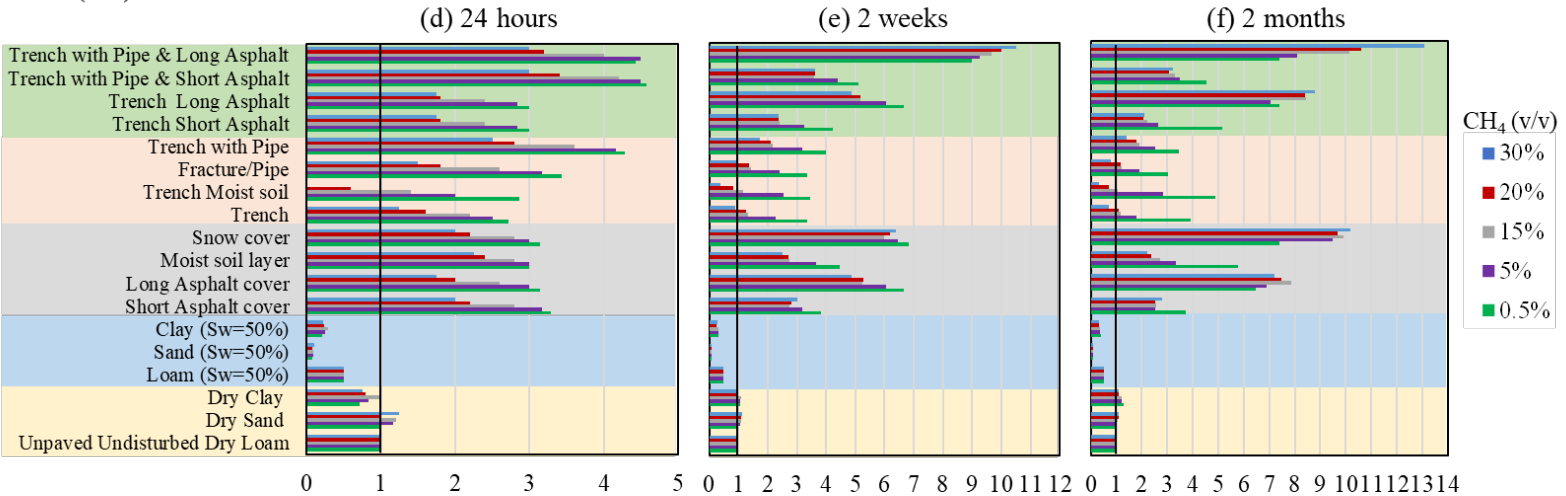
After comparing the variation in belowground NG plume shape as influenced by different surface and subsurface complexities, the overall NG migration extent and rate were compared by considering the spatial and temporal variation in the 0.5%, 5%, 15%, 20%, and 30% CH<sub>4</sub> (v/v) concentration contours. This comparison provides an understanding of the relative influence of different environmental complexities relative to a baseline scenario (unpaved, undisturbed dry loam soil). Results clarify critical complexities and provide a relative magnitude of influence by complexity.

Figure 17 and Figure 18 show the variation in relative maximum migration distance (D<sub>max</sub>) by the CH<sub>4</sub> plume 0.5%, 5%, 15%, 20%, and 30% CH<sub>4</sub> (v/v) contours for a 1 slpm (Figure 17) and 10 slpm (Figure 18) leak. Although a full description of the figures can be found in Appendix 6, the main findings are summarized here.

0.1 m (4 in) Below Ground Surface



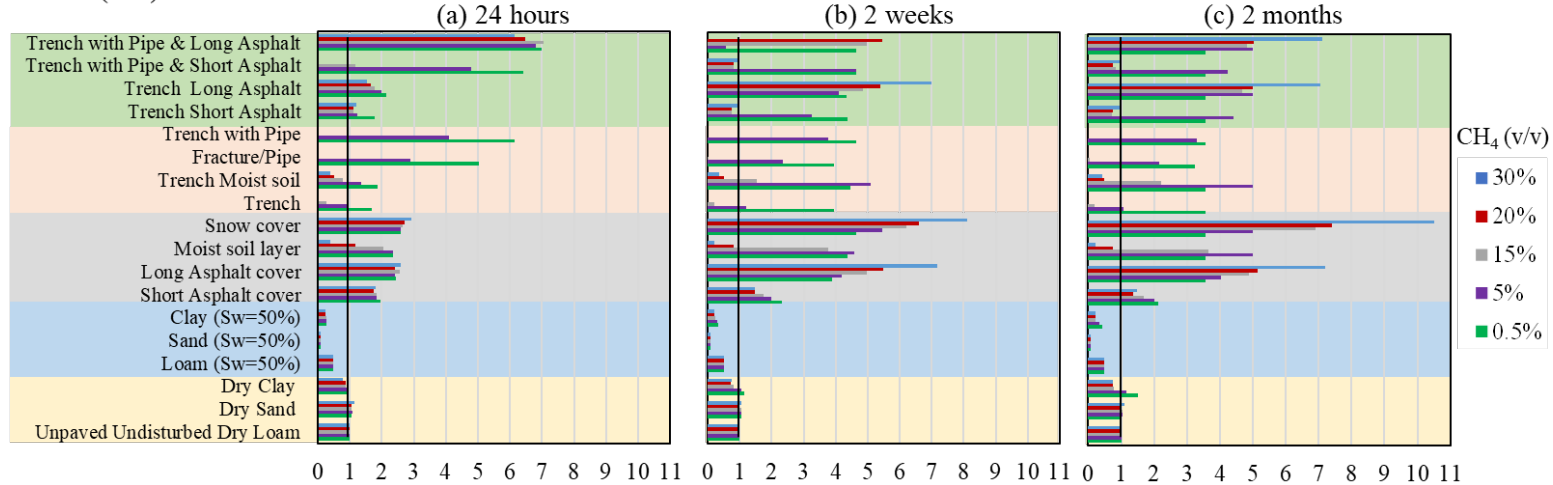
0.9 m (3 ft) Below Ground Surface



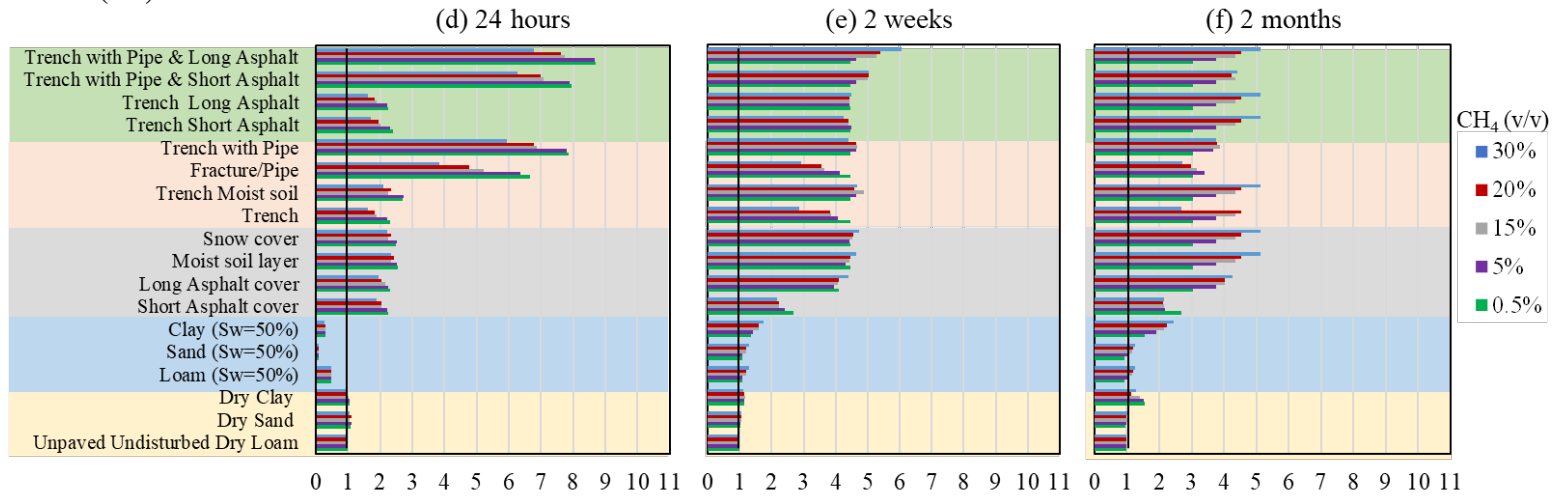
Travel Distance in Basecase terms

Figure 17: Variation in relative maximum migration distance ( $D_{max}$ ) by  $CH_4$  plume boundary, 5%, 15%, 20%, and 30%  $CH_4$  (v/v) contours for a 1 slpm leak at 0.1 m depth (a) 24 hours, (b) 2 weeks, (c) 2 months, after leak initiation and at 0.9 m depth (d) 24 hours, (e) 2 weeks, (f) 2 months, after leak initiation under different surface, and subsurface complexities. Here  $Sw=50\%$  represent that the soil is 50% moisture saturated. Vertical black line is the “unit” indicator for the basecase.

0.1 m (4 in) Below Ground Surface



0.9 m (3 ft) Below Ground Surface



Travel Distance in Basecase terms

Figure 18: Variation in relative maximum migration distance ( $D_{max}$ ) by  $CH_4$  plume boundary, 5%, 15%, 20%, and 30%  $CH_4$  (v/v) contours for a 10 slpm leak at 0.1 m depth (a) 24 hours, (b) 2 weeks, (c) 2 months, after leak initiation and at 0.9 m depth (d) 24 hours, (e) 2 weeks, (f) 2 months, after leak initiation under different surface, and subsurface complexities. Here  $Sw=50\%$  represent that the soil is 50% moisture saturated. Vertical black line is the “unit” indicator for the basecase.



For both the 1 and 10 slpm leaks (Figures 17 and 18), the lateral migration distances vary widely. Overall, the combined surface and subsurface complexity category followed by the surface complexity category report the highest migration rates over both short (24 hrs) and long (2 month) timelines. For a small leak (1 slpm) (Figure 17), the overall migration extent of the plume boundary (defined by 0.5% CH<sub>4</sub> (v/v)) increases by 5 times at 0.1 m depth and 13 times at 0.9 m depth, with an increase in subsurface complexity. Over longer periods of time (i.e. > 2weeks), a slow expansion of the overall plume boundary can be seen. In addition, gas accumulation close to the leak point is exhibited, resulting in increased migration extents of the 20% and 30% CH<sub>4</sub> (v/v). For the 10 slpm leak (Figure 18), the 0.5% (plume boundary) migrated 4 times at 0.1 m depth and 13 times at 0.9 m depth compared to the base case leak. Similarly to the 1 slpm leak, over time accumulation effects are shown (increased migration extents shown by 30% CH<sub>4</sub> (v/v) after 2 weeks or 2 months).

Figures 19 and 20 show the variation in the average CH<sub>4</sub> migration rate for the 0.5%, 5%, 15%, 20%, and 30% CH<sub>4</sub> (v/v) contours for a 1 slpm (Figure 19) and 10 slpm (Figure 20) leaks. For each subplot, the migration rates are presented by combining each individual scenario. For example, for the bar representing the 0.5% CH<sub>4</sub> (v/v) migration rate at 0.1 m BGD under combined surface and subsurface category (Figure 19a), the upper margin shows the maximum migration rate, the lower margin shows the minimum migration rate, and the dark like shows the average migration rate shown within the category. For small leaks (1 slpm) (Figure 19), the surface cover impacts the migration rate more than any other complexity. In the figure, one can follow the migration rate over time (e.g. 24 hrs to 2 months) and see a reduction over time. This decrease is greatest in the 30% contours but is also seen in the 0.5% contours as well.

When the leak rate increases to 10 slpm (Figure 20), the subsurface anomalies rather than the surface covers, dominate the migration rate impact. Overall the migration rates are higher than the 1 slpm leak scenarios and like the 1 slpm scenarios, decrease over time.

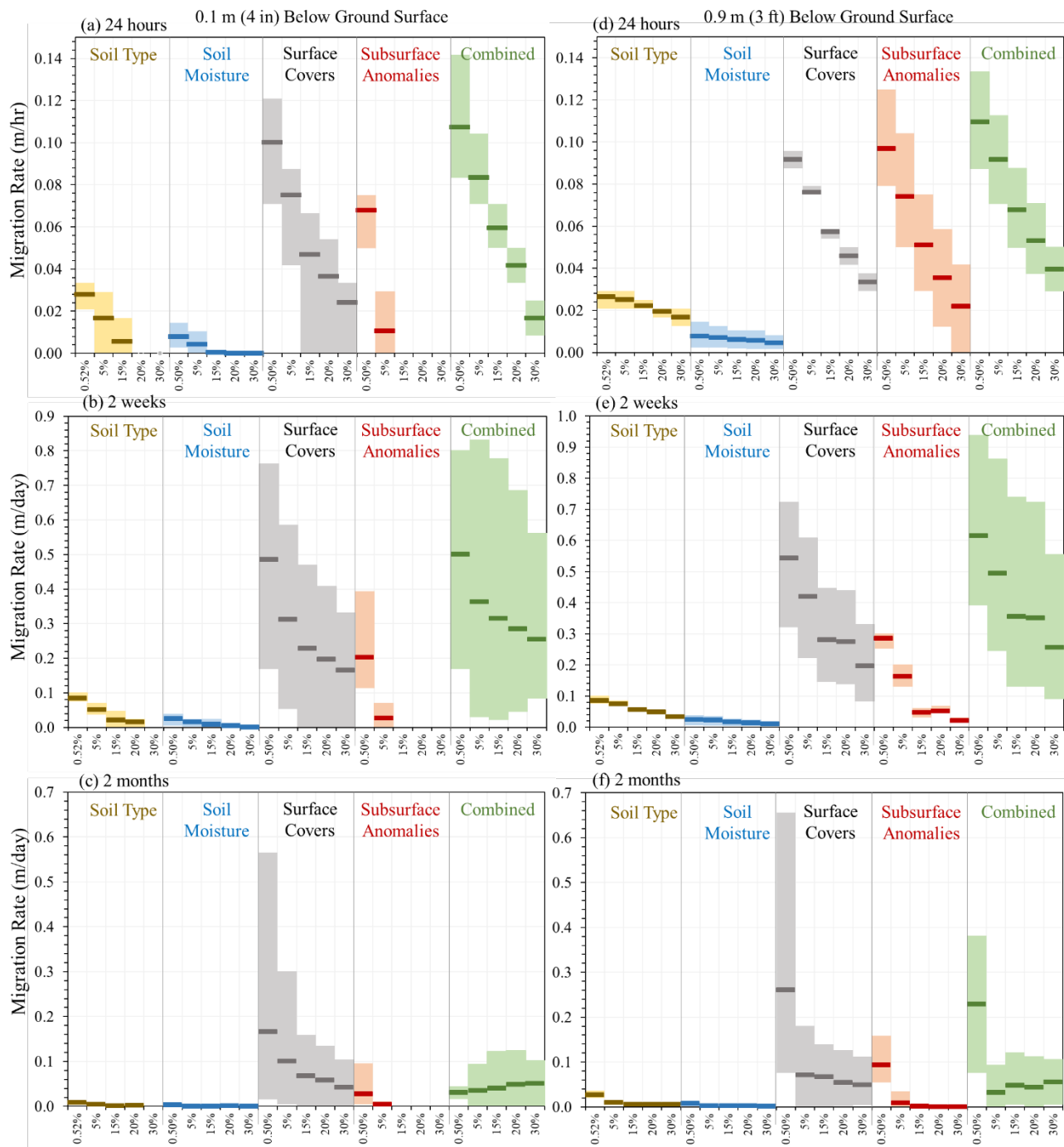


Figure 19: Variation in migration rate range by 0.5%, 5%, 15%, 20%, and 30% CH<sub>4</sub> (v/v) contours for a 1 slpm leak at 0.1 m depth (a) 24 hours, (b) 2 weeks, (c) 2 months after leak initiation and at 0.9 m depth (d) 24 hours, (e) 2 weeks, (f) 2 months after leak initiation under different surface, and subsurface complexities. Here, the bottom margin of each color box represents the minimum migration rate, the upper margin represents the maximum migration rate, and the dark line represents the average migration rate shown by each concentration contour under the respective category. Here Sw=50% represent that the soil is 50% moisture saturated.

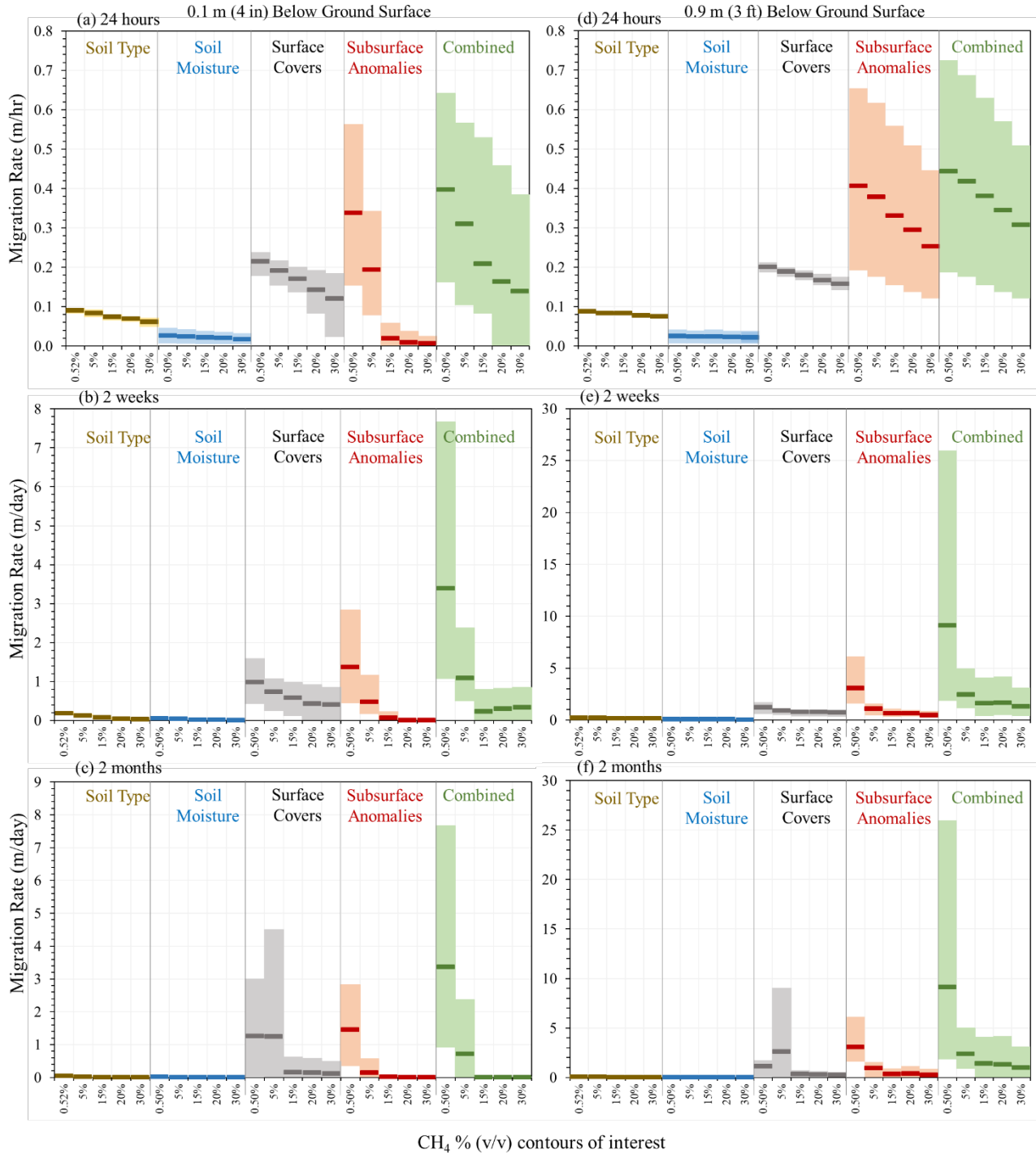


Figure 20: Variation in migration rate range by 0.5%, 5%, 15%, 20%, and 30% CH<sub>4</sub> (v/v) contours for a 10 slpm leak at 0.1 m depth (a) 24 hours, (b) 2 weeks, (c) 2 months after leak initiation and at 0.9 m depth (d) 24 hours, (e) 2 weeks, (f) 2 months after leak initiation under different surface, and subsurface complexities. Here, the bottom margin of each color box represents the minimum migration rate, the upper margin represents the maximum migration rate, and the dark line represents the average migration rate shown by each concentration contour under the respective category. Here  $S_w=50\%$  represents that the soil is 50% moisture saturated.

## 7.4 Long-term Behavior of Subsurface of NG Leaks

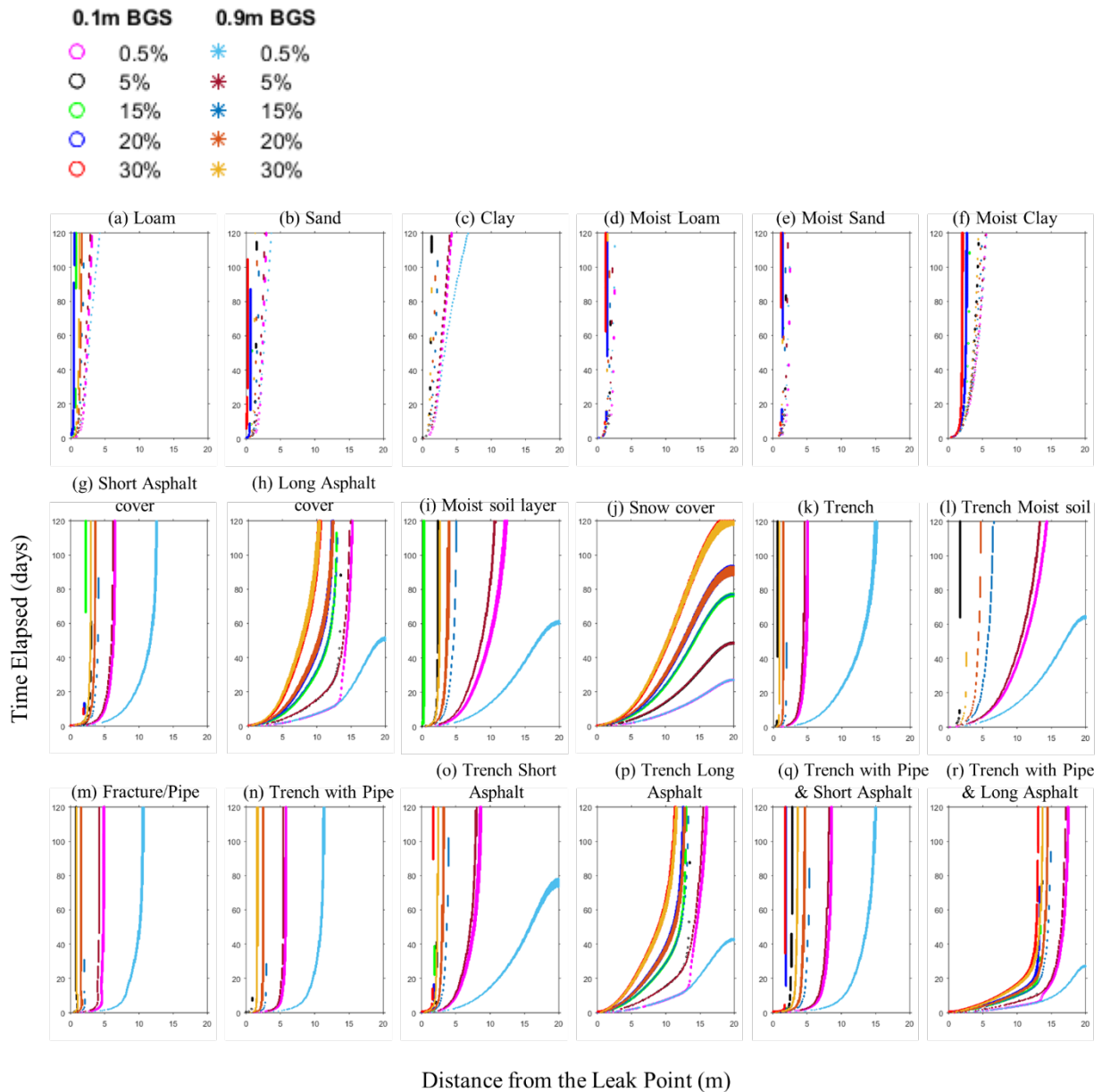


Figure 21: Variation in subsurface 0.5%, 5%, 15%, 20%, and 30%  $CH_4$  (v/v) contour migrations over time at 0.1 m and 0.9 m depths from a 1 slpm leak under different surface and subsurface complexities.

Figure 21 and Figure 22 show the behavior of the 1 slpm and 10 slpm leaks, respectively, over a period of 120 days. In general, the plumes expand slowly over time and reach a steady state except for the scenarios under surface covers. This can especially be seen in the long asphalt cover cases. Importantly, since the snow case is a continuous cover, the concentration contours continued to migrate without ever stabilizing at a certain distance.

Overall, under different subsurface complexities, concentration contours  $>5\%$   $\text{CH}_4$  (v/v) reached a steady state close to the leak point while the 5% and 0.5%  $\text{CH}_4$  (v/v) contours continue to expand laterally away from the leak location. When the surface and subsurface complexities are combined, contour migration patterns follow a trend mimicking a combination of the surface complexity category and the subsurface complexity category.

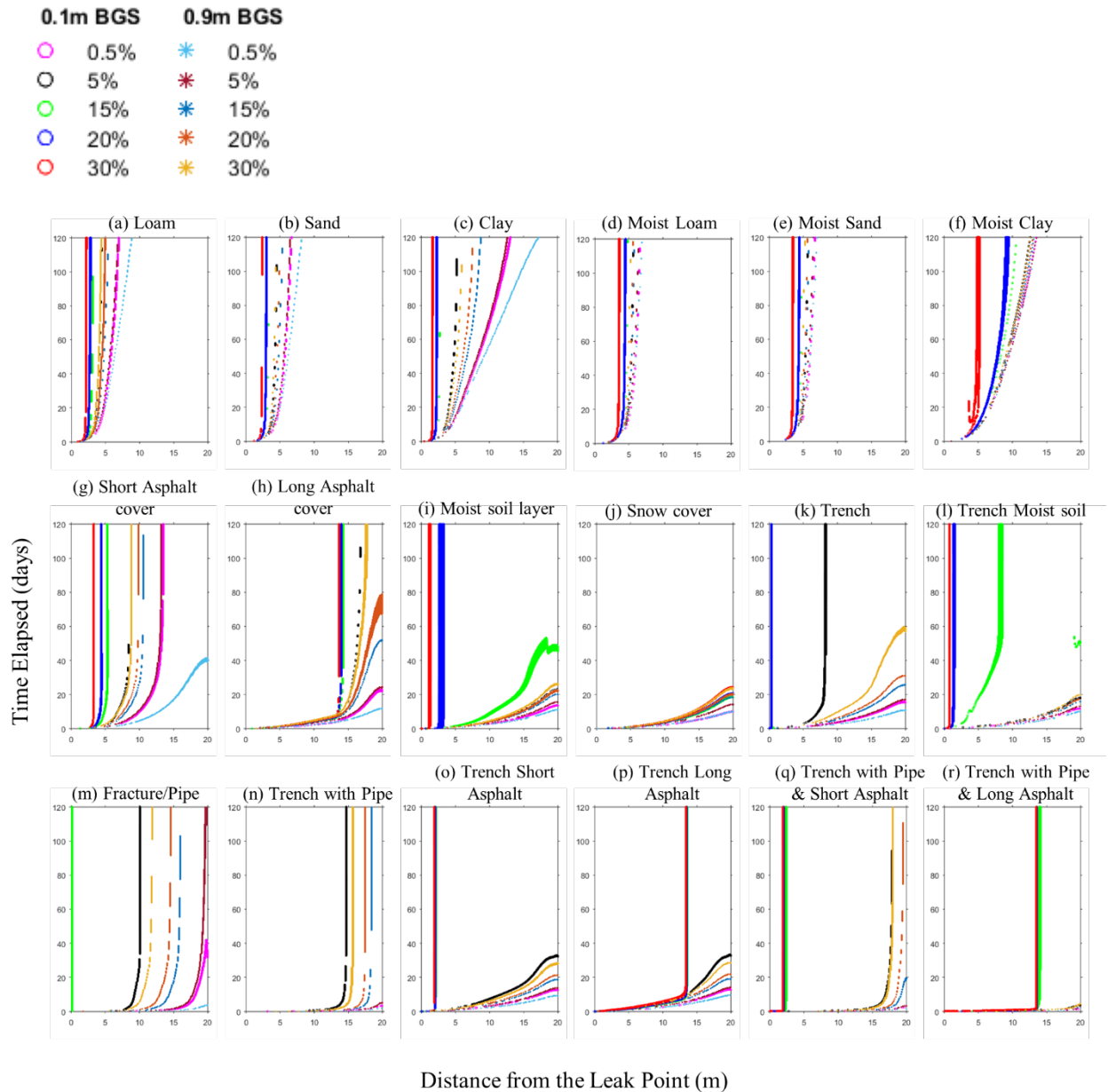


Figure 22: Variation in subsurface 0.5%, 5%, 15%, 20%, and 30%  $\text{CH}_4$  (v/v) contour migrations over time at 0.1 m and 0.9 m depths from a 10 slpm leak under different surface and subsurface complexities.

For large leaks (Figure 22), the bulk expansion of the plume seen during the initial periods (approx. 24 hrs) slow down over time. Similar to the small leak scenarios, the gas continues to migrate away from the leak point under surface covers, with higher (e.g. >15% CH<sub>4</sub> (v/v)) contours reaching the edge of the surface cover.

## 7.5 Key Findings

- **Complexity impacting migrate rate and extent:** relative to the base case presented here, the conditions having the most impact on CH<sub>4</sub> migration rate and extent are (from highest to lowest): 1) subsurface fractures or gaps due to utility pipelines, 2) disturbed soil in trenches, 3) surface covers, 4) soil moisture, and 5) soil type, where soil type exhibits little influence compared to factors 1-4. Additionally, the combination of these complexities can compound and increase the influence further.
- **Soil type:** Changes in soil type (loam, sand, or clay) has little effect on the overall 15%, 5%, and 0.5% CH<sub>4</sub> (v/v) contours that are required for leak classification and first responder operations compared the other complexities. However, changes in soil type changes the overall spatial distribution of CH<sub>4</sub> during a leak event and the long-term venting of the CH<sub>4</sub> as it returns to background level concentrations. For example, loam soil results in a wide concentration gradient from the leak point towards the plume boundary versus a narrow concentration gradient towards the plume boundary for clay soil.
- **Surface condition:** In the leak scenarios associated with a change in surface condition from unpaved to paved, snow covered, or moisture cap, the gas accumulation under the surface condition creates a wider plume with CH<sub>4</sub> saturation extending to a large distance and a narrow concentration gradient towards the plume boundary. For the conditions tested, the resulting plume increases the gas migration extent by 3 times that of an unpaved leak within the first 24 hours and > 5 times that of an unpaved leak within a 2-month period for small leak rates. The migration extent increases by 2.5 times for the first 24 hours and > 50 times after 2 months for a large leak.

- **Subsurface condition:** In the leaks associated with subsurface anomalies (fracture, gaps due to utility pipelines, and soil disturbance), CH<sub>4</sub> concentrations are dispersed across a large area, creating wider concentration gradients. Therefore, leaks associated with subsurface anomalies result in 4-times far migration extents in 24 hours and 5-times further migration extents over a 2-month period for small leaks compared to a similar leak under Unpaved Undisturbed Dry Loam soil conditions. For the conditions tested, migration extent can be increased up to 4-times and > 5-times respectively after 24 hours and 2 months for a large leak.
- **Combined Surface and Subsurface complexities:** The leaks associated with combined surface and subsurface complexities create critical gas migration extents and rates, resulting in migration extents 5 times greater in 24 hours and 30-times greater after 2 months for small leaks, compared to similar leaks under base case conditions. For large leak conditions, this increases to 8 times larger migration extents after 24 hours, and > 5-times larger migration extents after 2 months compared to a similar large leak in Unpaved Undisturbed Dry Loam conditions. During scenarios with trenches or buried pipes covered by asphalt layers, the pipeline gap followed by disturbed soil in the trench dominates gas migration over the surface cover.

## **8. Deliverable 15: Underground natural gas pipeline leak: recommendations for first responders**

### **8.1 Objective:**

The objective of this deliverable is to link key scientific findings on the transient behavior of NG with first responder practice. This first included a review of first responder pipeline emergency response guidelines and local fire authority operational directives, and discussions with first responders to understand their protocols. This was followed by linking the scientific findings from the 150 controlled release experiments and parallel numerical modeling to first responder understanding and practices. Background for each finding, scientific description, and the detailed explanations for each recommendation can be found in Appendix 7: Underground Natural Gas Pipeline Leak Behavior: Connecting gas migration understanding to first responder protocols.

### **8.2 Key Findings**

- Changes in surface conditions impact how far and how fast the gas travels below the ground. Moisture, snow and asphalt can block gas from escaping the surface and result in gas moving both downwards and outwards away from the leak location. In the presence of asphalt, snow or rain (wet surface), gas can spread up to 3 to 4 times further and 3.5 times faster than the equivalent leak scenario under dry soil conditions.
- The methane surface expression is not representative of the size of the belowground leak. For example, under wet soil conditions, negligible methane concentrations are found at the surface while the largest accumulation of gas is found at shallow depths below the ground surface (BGS).
- An increase in leak rate does not proportionally increase the gas migration rate and distance. High leak rates result in faster, and initially further gas migrations for the high concentration contours but has little influence on the low concentration contours farther from the leak location.
- Under transient conditions, transport is faster and initially further for the high concentration contours. However, over time when steady or a quasi-steady state is achieved, smaller and larger leak rates may result in similar areas of influence. This implies that for established unresolved leaks that have persisted over time, the locations



commonly considered unsafe for high leak rate scenarios should also be considered for unresolved low leak scenarios.

- Leak termination does not immediately remove the high belowground concentrations; gas can retain at concentrations above x LEL up to 14 days when asphalt, snow or moist soil conditions are present. Therefore, effort should be taken to vent the soil post termination.
- Because gas retains within the soil with reduced venting due to the snow, wet and/or asphalt conditions, gas can continue to migrate away from the leak source. This is particularly critical for Grade 1 (hazardous) leaks, which often start suddenly due to failure of underground infrastructure or excavation accidents. In these cases, the gas plume will be established quickly and may continue to evolve even after leak termination.
- While natural gas is composed mostly of methane, the ratio of other gases (e.g. ethane, propane) affects the gas behavior as it moves underground. As the gas density increases, the potential for gas build up underground increases and lateral migration increases. Higher ethane and propane composition increase migration distance by 3 times and retention duration by 6 times.
- The severity of a leak may be underestimated in some conditions as surface and therefore atmospheric concentrations do not always give a clear indication of how large a leak could be. Therefore, a hot zone of 300' radius should be established for any leak where the threshold limit value of 20% LEL is observed in open spaces
- A hot zone should be considered even if the threshold of 20% LEL has not been exceeded when any of the following is observed at the leak site:
  - Waterlogged soil
  - Snow cover
  - Ice on the surface
  - Asphalt on surface
  - High winds
  - Very sunny conditions
  - Nighttime

## 9. Deliverable 17: Project Outputs

### 9.1 Objective:

To present the scientific understanding and the implications to NG operators and first responders in a systematic and readily available manner. The Project outputs include 12 Peer Reviewed Publications (8 published and 4 in review), 23 Conference presentations and Posters, 2 invited presentations, 3 METEC Research Alerts, and 3 Media Reports. Hyperlinks are provided when available to the publication/presentation.

### 9.2 Peer Reviewed Publications/ Proceedings

Publication	Objective	Results/Importance	Data Repository Link
1. Jayarathne, J. R. R. N., Kolodziej, R. S., Riddick, S. N., Zimmerle, D. J., & Smits, K. M. (2024). Flow and Transport of Methane from Leaking Underground Pipelines: Effects of Soil Surface Conditions and Implications for Natural Gas Leak Classification. <i>Environmental Science and Technology Letters</i> , <i>In review</i>	To identify the impact of diverse surface conditions (snow, rain, and asphalt) on belowground CH <sub>4</sub> transport fro NG pipeline leaks, impacting both safety and environmental risks assessment.	<ul style="list-style-type: none"> <li>- Changes I the surface condition impact the gas migration distance and rate belowground. In the presence of asphalt, snow, or moist soil layers can spread the gas up to 3 to 4 times farther and 3.5 times faster than an equivalent leak under dry soil conditions.</li> <li>- Terminating the gas supply does not immediately remove high belowground concentrations and hence ignitable conditions.</li> </ul>	Jayarathne,J.R.R.N.; Kolodziej, R.S.; Riddick, Stuart N; Zimmerle, D.J.; Smits, Katheen M, 2023, "Replication Data for: Flow and Transport of Methane from Leaking Underground Pipelines: Effects of Soil Surface Conditions and Implications for Natural Gas Leak Classification", <a href="https://doi.org/10.18738/T8/MQ5AQR">https://doi.org/10.18738/T8/MQ5AQR</a> , Texas Data Repository, V1, UNF:6:gHmaGMscJ7Vx3gaNvMJnLA== [fileUNF]

<p>2. Jayarathne, J. R. R. N., Kolodziej, R. S., Riddick, S. N., Zimmerle, D. J., &amp; Smits, K. M. (2023). Influence of soil-gas diffusivity on expansion of leaked underground natural gas plumes and application on simulation efforts. <i>Journal of Hydrology</i>, 625(PB), 130049. <a href="https://doi.org/10.1016/j.jhydr.2023.130049">https://doi.org/10.1016/j.jhydr.2023.130049</a></p>	<p>To evaluate the performance of diffusivity parametric functions used in the field scale models of NG leakage to represent gas migration extent and changes over time.</p>	<ul style="list-style-type: none"> <li>- The study presented the importance of considering soil type/structure and moisture variation in large-scale gas migration simulations.</li> <li>- Results showed that selection of a Diffusivity Parametric Function plays a significant role (1) when the soil structural complexities arise from soil disturbance and moisture variations (2) after terminating the leak, where advection effect diminishes, and diffusion dominates, (3) when defining the edge of the plume where diffusion dominates the far field migration and slow migration of gases.</li> </ul>	<p>NA</p>
<p>3. Mbua, M., Riddick, S. N., Tian, S., Cheptonui, F., Houlihan, C., Smits, K. M., &amp; Zimmerle, D. J. (2023). Using controlled subsurface releases to investigate the effect of leak variation on above-ground natural gas detection. <i>Gas Science and Engineering</i>, 120(July), 205153. <a href="https://doi.org/10.1016/j.jgsce.2023.205153">https://doi.org/10.1016/j.jgsce.2023.205153</a></p>	<p>To investigate the effects of gas composition, leak rate, and leak depth on the aboveground plume for a subsurface leak to inform leak detection using above-ground surveys</p>	<ul style="list-style-type: none"> <li>- The study shows that the leak characteristics further complicate leak detection and that the downwind plume may not simply not exist due to the leak depth or the gas composition</li> <li>- Encountering a plume from a wet gas leak only detectable close to the surface could give a false impression of a small leak, resulting in non-prioritization of the leak repair.</li> </ul>	<p>Mbua, Mercy et al. (2023). Data from: Using controlled subsurface releases to investigate the effect of leak variation on above-ground natural gas detection [Dataset]. Dryad. <a href="https://doi.org/10.5061/dryad.ncjsxkt15">https://doi.org/10.5061/dryad.ncjsxkt15</a></p>

<p>4. Cheptonui, F., Riddick, S. N., Hodshire, A. L., Mbua, M., Smits, K. M., &amp; Zimmerle, D. J. (2023). Estimating the Below-Ground Leak Rate of a Natural Gas Pipeline Using Above-Ground Downwind Measurements: The ESCAPE-1 Model. <i>Sensors (Basel, Switzerland)</i>, 23(20). <a href="https://doi.org/10.3390/s23208417">https://doi.org/10.3390/s23208417</a></p>	<p>To investigate whether CH<sub>4</sub> mixing ratios from an industry-standard instrument can be used to infer a pipeline's belowground gas leak rate.</p>	<ul style="list-style-type: none"> <li>- Investigated the environmental conditions in which lower-cost, industry standard CH<sub>4</sub> detectors could be used to quantify leak rates from subsurface NG pipeline leaks installed in rural environments.</li> <li>- CH<sub>4</sub> data measured using a CH<sub>4</sub> detector can be used to calculate leak rates between 0.2 and 0.8 kg CH<sub>4</sub> h<sup>-1</sup> at wind speeds above 2 ms<sup>-1</sup> when the pipeline is traveling through the native soil.</li> </ul>	<p>The data sets for this study are found in the reference: Fancy Cheptonui; Riddick N. Stuart; Anna Hodshire; Mercy Mbua; Kathleen M. Smits; Daniel J. Zimmerle; Replication Data for Estimating the below-ground leak rate of a Natural Gas pipeline using above-ground downwind measurements: THE ESCAPE<sup>-1</sup> MODEL, <a href="https://datadryad.org/stash/share/hrNNi7QftejUvL LT2Nahi2tM26ilVLk36 Qe8NYAToM">https://datadryad.org/stash/share/hrNNi7QftejUvL LT2Nahi2tM26ilVLk36 Qe8NYAToM</a> (accessed on 6 September 2023), Dryad data repository.</p>
<p>5. Lo, J., K.M. Smits, Y. Cho, G.P. Duggan, S.N. Riddick. 2023. Quantifying Non-steady State Natural Gas Leakage from the Pipelines Using an Innovative Sensor Network and Model for Subsurface Emissions -InSENSE, Environmental Pollution. <i>ENPO 122810</i>.</p>	<p>To introduce an innovative approach to quantify underground NG leak rates under non-steady conditions using an inverse gas migration model and surface near-real-time and low-cost CH<sub>4</sub> detector network.</p>	<ul style="list-style-type: none"> <li>- The study developed and tested a model based on concept of coupling soil and atmospheric resistance, key environmental parameters, and limited belowground and surface CH<sub>4</sub> concentration measurements to estimate the non-steady state CH<sub>4</sub> leak rates over time.</li> <li>- Belowground near surface CH<sub>4</sub> concentration is an important factor in leak rate estimates as the surface expression does not necessarily</li> </ul>	<p>NA</p>

<a href="https://doi.org/10.1016/j.envpol.2023.122810">https://doi.org/10.1016/j.envpol.2023.122810</a>		define the belowground plume location/behavior.	
6. Tian, S., S.N. Riddick, Y. Cho*, C.S. Bell, D.J. Zimmerle, K.M Smits. 2022. Investigating detection probability of mobile survey solutions for natural gas pipeline leaks under different atmospheric conditions. <b>Environmental Pollution</b> . <a href="https://doi.org/10.1016/j.envpol.2022.120027">https://doi.org/10.1016/j.envpol.2022.120027</a>	To explore the effectiveness of using limited surface and aboveground CH <sub>4</sub> mole fraction data as inputs to a near-filed dispersion model to calculate CH <sub>4</sub> emissions from subsurface pipeline leaks under realistic conditions.	<ul style="list-style-type: none"> <li>- The work tested an approach to estimate CH<sub>4</sub> emission rates compared to known leak rates from subsurface pipeline leaks under realistic conditions.</li> <li>- Results confirmed that the mean normalized CH<sub>4</sub> mole fraction increases as the atmosphere transitions from PG stability classes A (extremely unstable) – G (extremely stable).</li> <li>- Findings emphasize that a certain amount of data are necessary to have an estimate that can reflect the true subsurface leak rates.</li> </ul>	Available on Request
7. Tian, S., K.M. Smits, Y. Cho*, S.N. Riddick, D.J. Zimmerle, A. Duggan. 2022. Estimating methane emissions from underground natural gas pipelines using an atmospheric dispersion-based method. <b>Elem Sci Anthr</b> . <a href="https://doi.org/10.1525/elementa.2022.00045">https://doi.org/10.1525/elementa.2022.00045</a>	Assess the effectiveness of a simple dispersion-based method for estimating NG leakage rates from underground pipelines and inform emission estimate methods	<ul style="list-style-type: none"> <li>- Methane concentration evolves with an obvious temp-spatial variability in the sub-diurnal scale</li> <li>- Dispersion-based method provides a cost effective, alternative tool to estimate the pipeline leaks within a certain accuracy, using the typical measurements from a general walking or driving survey</li> </ul>	Data sets for this research are available in the in-text data citation reference: Tian, Shanru; Smits, Kathleen M.; Cho, Younki; Riddick, Stuart; Zimmerle, Daniel; Duggan, Aidan. 2022. Replication data for estimating methane emissions from underground natural gas pipelines using an atmospheric dispersion-based method,

			<a href="https://doi.org/10.18738/T8/UAO5XX">https://doi.org/10.18738/T8/UAO5XX</a> , Texas Data Repository.
8. Riddick, S. N., Bell C., Duggan, A., Vaughn, T. L., Smits, K. M., Cho, Y., Bennett, K. E. and Zimmerle, D. J. (2021) Modelling temporal variability in the surface expression above a methane leak: The ESCAPE model. Journal of Natural Gas Science and Engineering. <a href="https://doi.org/10.1016/j.jngse.2021.104275">https://doi.org/10.1016/j.jngse.2021.104275</a>	Investigate the effects of soil properties on methane concentration and migration distance from leaking underground NG pipelines	<ul style="list-style-type: none"> <li>- Methane migration in the subsurface was seen to be predominantly affected by soil moisture and to a lesser extent soil texture</li> <li>- Water-induced tortuosity affected distribution of the gas which resulted in elevated methane concentrations near the leak location</li> <li>- Soil moisture is not a considered parameter when monitoring or grading NG leaks which can change the spread of the gas overtime</li> </ul>	NA
9. Cho, Y.*; K.M. Smits, N.L. Steadman, B.A. Ulrich*, C.S. Bell, D.J. Zimmerle, 2022, A closer look at underground natural gas pipeline leaks across the United States, <b>Elementa: Science of the Anthropocene</b> , <a href="https://doi.org/10.1525/elementa.2021.00095">https://doi.org/10.1525/elementa.2021.00095</a>	Provide guidance to the interwoven contribution of key atmospheric variability on the surface presentation of the leak	<ul style="list-style-type: none"> <li>- Atmosphere has a profound effect on methane concentrations measured at the surface where wind speed, surface roughness length, and the atmospheric stability has the most significant affect</li> <li>- Larger gas leaks could have advection occur fast enough, removing methane from the subsurface to the atmosphere,</li> </ul>	Cho, Younki; Smits, Kathleen M.; Steadman, Nathaniel L.; Ulrich, Bridget A.; Bell, Clay S.; Zimmerle, Daniel J., 2022, "Replication Data for: A Closer Look at Underground Natural Gas Pipeline Leaks Across the United States", <a href="https://doi.org/10.18738/T8/32VPN0">https://doi.org/10.18738/T8/32VPN0</a> , Texas Data Repository, V1

<p>10. Jayarathne, J. R. R. Navodi, K.M. Smits, S.N. Riddick, D. J. Zimmerle, Y. Cho, M. Schwartz, F. Cheptonui, K. Cameron, P. Ronney, 2022, Understanding Mid-to Large Underground Leaks from Buried Pipelines as Affected by Soil and Atmospheric Conditions –Field Scale Experimental Study. <b>Proceedings from the Pipeline Research Council International (PRCI) REX2022 Meeting.</b> (presentation and proceedings)</p>	<p>To validate the methods developed for experimental and numerical determination of belowground NG migration extent and rate</p>	<p>NA</p>	<p>NA</p>
<p>11. Tian, S., S.N. Riddick, M. Mbua, Y. Cho*, D.J. Zimmerle, K.M. Smits. 2022. Improving the efficacy of leak survey methods using 3D plume measurements. <i>In review</i></p>	<p>To identify how the effects of the atmosphere variability impact the gas plume development in the atmosphere and most importantly, how we can use this understanding to inform and optimize leak survey protocol parameters.</p>	<p>- Filed-scale belowground leak experiments and 3D gas dispersion modeling based on OpenFOAM were performed to investigate the impact of environmental variability on CH<sub>4</sub> plume development and the selection of common leak survey parameters including the maximum effective survey speed, height above the ground, and the downwind from the leak center. For walking, driving and UAV survey</p> <p>- Results showed that 3D plume shape and size decreases with as increase in atmospheric stability from PG A (extremely unstable) to PG G (extremely stable).</p>	<p>-</p>

<p>12. Riddick, S. N., Cheptonui, F., Tian, S., Jayarathne, J. R. R. N., Mbua, M., Smits, K. M. and Zimmerle, D. J. Reconciling above and below ground methane concentration measurements for subsurface emissions of wet and dry natural gas. <i>In preparation.</i></p>		-	-
<p>13. Jayarathne, J. R. R. N., Kolodziej, R. S., Riddick, S. N., Zimmerle, D. J., &amp; Smits, K. M. (2024). Differential Subsurface Methane Migrations Influenced by Surface and Subsurface Structural Complexities. <i>In preparation</i></p>	<p>1) determine NG migration extent and rate under individual surface and subsurface leak environment complexities 2) determine the relative importance of each complexity relative to a selected base case (a leak under no surface and subsurface complexities) 3) determine the combinations that lead to critical leaked NG migrations.</p>	<p>- the order of influence by surface and subsurface complexities on leaked NG migration starting from the highest, 1) subsurface fractures or gaps due to utility pipelines, 2) disturbed soil in trenches, 3) surface covers, 4) soil moisture and 5) soil types with little to no influence. Hence, the combinations can increase the influence further. - leaks associated with subsurface complexities result in 4-times far migration extensions in 24 hours and 5-times far migration extents in 2 months for small leaks compared to a similar leak under Unpaved Undisturbed Dry Loam soil conditions. Migration extent can be increased up to 4-times and &gt; 5-times respectively for 24 hours and 2 months for a large leak.</p>	- NA



### 9.3 Conference Presentation and Posters

1. Jayarathne J.R.R.N, R.S Kolodziej IV, Y. Cho, S.N. Riddick, D.J. Zimmerle, and K.M. Smits. (2023). Unraveling Natural Gas Migration Rate and Extent from Leaking Underground Pipelines under Varying Environmental Conditions. **CH<sub>4</sub> Connections-The Methane Emissions Conference, 4-5 October 2023**, Fort Collins-Colorado
2. Tian, S., S. N. Riddick, M. Mbua, Y. Cho, A. Hodshire, Y Zhang, D. Zimmerle, K. M Smits. (2023). Improving the Efficiency of Mobile Leak Survey Methods Using 3D Plume Modeling and Measurements. **CH<sub>4</sub> Connections-The Methane Emissions Conference, 4-5 October 2023**, Fort Collins-Colorado
3. Lo, J., K.M. Smits, Y. Cho, J. Duggan. (2023). Quantifying Non-steady State Natural Gas Leakage from the Pipelines using an Innovative Sensor Network and Model for Subsurface Emissions. **CH<sub>4</sub> Connections-The Methane Emissions Conference, 4-5 October 2023**, Fort Collins-Colorado
4. Kolodziej, R., S. Tian, V. Rao, K. M Smits, A. Hodshire, D. Zimmerle. (2023). Assessing the Impact of Environmental and Pipeline Conditions on Subsurface Natural Gas Pipeline Leak Detection. **CH<sub>4</sub> Connections-The Methane Emissions Conference, to be held on 4-5 October 2023**, Fort Collins-Colorado
5. Smits, K.M., GHG Reduction Opportunities through Detection and Quantification of Belowground Natural Gas Pipeline Leaks, **Texas Society of Professional Engineers (TSPE) Annual Meeting, Dallas TX, May 11, 2023**, Invited presentation.
6. Smits, K.M., GHG Reduction Opportunities through Detection and Quantification of Belowground Natural Gas Pipeline Leaks, **PHMSA's Accident Investigation Division Meeting, Washington, D.C., April 25, 2023**, Invited presentation.
7. Jayarathne J.R.R.N, R.S Kolodziej IV, Y. Cho, S.N. Riddick, D.J. Zimmerle, and K.M. Smits. 2023. Unraveling Natural Gas Migration Rate and Extent from Leaking Underground Pipelines under Varying Environmental Conditions. SMU Moody

School of Graduate & Research Studies-Research and Innovation Week, 20-25 March, 2023 (Poster)

8. Jayarathne J.R.R.N, R.S Kolodziej IV, Y. Cho, S.N. Riddick, D.J. Zimmerle, and K.M. Smits. 2023. Belowground Migration Rate and Extent of Leaked Natural Gas as Influenced by Varying Surface Conditions: Experimental and Numerical Study. SFB1313 – Interface-Driven Multi-Field Process in Porous Media, 26-29 March 2023 (Poster), Stuttgart, Germany.
9. Jayarathne J.R.R.N, R.S Kolodziej IV, Y. Cho, S.N. Riddick, D.J. Zimmerle, and K.M. Smits. 2022. Unraveling Natural Gas Migration Rate and Extent from Leaking Underground Pipelines under Varying Environmental Conditions. **2022 AGU Fall Meeting, 12 -16 December 2022**, Chicago, Illinois. (poster)
10. Jayarathne J.R.R.N, R.S Kolodziej IV, Y. Cho, S.N. Riddick, D.J. Zimmerle, and K.M. Smits. 2022. Unraveling Natural Gas Migration Rate and Extent from Leaking Underground Pipelines under Varying Environmental Conditions. **CH4 Connections conference, October 20-21, 2022**, Fort Collins, Colorado. (poster)
11. Tian, S., S.N. Riddick, M. Mbua, Y. Cho, D.J. Zimmerler, K.M. Smits. 2022. Improving the efficacy of leak survey methods using 3D plume measurements. **2022 AGU Fall Meeting**, 12 -16 December 2022, Chicago, Illinois. (poster)
12. J. Lo, K.M. Smits, Y. Cho, J. Duggan, S. Riddick, Utilizing the Near Real-Time Methane Detector Network to Study and Quantify Underground Natural Gas Leakage from the Pipeline, **CH4 Connections conference**, Oct 20-21, 2022 (poster)
13. Mbua, M., S.N. Riddick, S. Tian, , F. Cheptonui, H. Cade, Y. Cho, K.M. Smits, and D.J. Zimmerle. 2022 Using controlled subsurface leak experiments to improve leak detection solutions' protocol. The ninth annual **CH4 Connections conference**, October 20-21, 2022, Fort Collins, Colorado. (poster)
14. Lo, J., K.M. Smits, Y. Cho, J. Duggan, S. Riddick, Utilizing the Near Real-Time Methane Detector Network to Study and Quantify Underground Natural Gas

Leakage from the Pipeline, **American Geophysical Union Fall Meeting**, Dec 2022 (poster)

15. Tian, S., S.N. Riddick, M. Mbua, Y. Cho, D.J. Zimmerler, K.M. Smits. 2022. Improving the efficacy of leak survey methods using 3D plume measurements. The ninth annual **CH<sub>4</sub> Connections conference**, October 20-21, 2022, Fort Collins, Colorado.(poster)
16. Cho, Y., J. H. Lee, J. Lo, J. Duggan, K. M. Smits, and D. Zimmerle. "Natural gas fugitive leak detection and quantification using a continuous methane emission monitoring system and a simplified model" **AGU 2022 Fall meeting**(poster)
17. Jayarathne J R R N, Y Cho, and K M Smits. 2021. Sensor-based Determination of Underground Natural Gas Migrations Influenced by Near-surface Atmospheric Fluctuations. **American Geophysical Union Fall 2021 meeting. 13-17 December 2021**. New Orleans. Louisiana. Abstract ID 909733
18. J R R N Jayarathne, Y Cho, and K M Smits. 2021. Soil-Gas Diffusivity Driven Expansion of Underground Natural Gas Plumes. ASA, CSSA, SSSA INTERNATIONAL ANNUAL MEETING. 7-10 November 2021. Salt Lake City- Utah.
19. Jayarathne, J.R.R.N, Y Cho, K.M. Smits, S Riddick, and D. Zimmerle. 2021. Methods for Understanding Mid to Large Underground Natural Gas Leaks. CH<sub>4</sub> Connections- The Methane Emissions Conference, 12-13 October 2021
20. Riddick (2022) Looking for the UPSIDE to natural gas pipeline leaks. The Great Escape: detecting and measuring gas leaks. Gas Analysis and Sensing Group, 83rd GASG Colloquium. 1st December 2022. City, University of London, London, UK (Invited).
21. Riddick et al. (2022) Using controlled subsurface emission experiments to improve leak detection solutions' protocol: The UPSIDE project. AGU Fall Meeting 2022

22. Riddick (2021) PHMSA Pipeline Safety: Pipeline Leak Detection, Leak Repair and Methane Emission Reductions. PHMSA Public Meeting, April 2021 (Invited).
23. Riddick et al. (2020) Modelling temporal variability in the surface expression above a methane leakage: The ESCAPE model. AGU Fall Meeting 2020.

#### 9.4 Invited Presentations

1. Smits, K.M., GHG Reduction Opportunities through Detection and Quantification of Belowground Natural Gas Pipeline Leaks, EPA Region 6 Science Council Seminar, Dallas TX, Sept 12, 2023, Invited presentation.
2. Smits, K.M., GHG Reduction Opportunities through Detection and Quantification of Belowground Natural Gas Pipeline Leaks, TX ASCE Science Seminar Series, July 11, 2023, Dallas TX, Invited presentation.
3. Smits, K.M., GHG Reduction Opportunities through Detection and Quantification of Belowground Natural Gas Pipeline Leaks, PHMSA's Accident Investigation Division Meeting, Washington, D.C., April 25, 2023, **(Invited Presentation)**.
4. Smits, K.M., GHG Reduction Opportunities through Detection and Quantification of Belowground Natural Gas Pipeline Leaks, SMU Department of Mechanical Engineering Seminar Series, March 1, 2023, **(Invited Presentation)**.
5. Smits, K.M. Quantification of anthropogenic methane sources through measurement studies: Finding targets for mitigation, SMU Earth Science Seminar Series, Jan 27, 2023 **(Invited Presentation)**.
6. Smits, K.M. Unraveling the Influence of Environmental Conditions on Natural Gas Pipeline Leak Behavior, Center for Energy and Environmental Resources (CEER), The University of Texas at Austin, March 7, 2022 **(Invited Presentation)**
7. Smits, K.M., Tools for Predicting Underground Natural Gas Migration and Mitigating its Occurrence/Consequence, School of Global Environmental Sustainability, Colorado State University, Dec 6, 2021 **(Invited Presentation)**.
8. Smits, K.M., Tools for Predicting Underground Natural Gas Migration and Mitigating its Occurrence/Consequence, American Gas Association, July 22, 2021 **(Invited Presentation)**.

9. Smits, K.M, Integrating social and technical understanding in development work – lessons from the field. Engineers Without Borders, The University of Texas at Arlington Student Chapter, March 10, 2021 (**Invited Presentation**).
10. Smits, K.M., Y. Cho, S. Tian, S. Riddick, B.A. Ulrich and D.J. Zimmerle, Novel Approaches to Estimate Natural Gas Emissions from Underground Pipelines using Surface and Atmospheric Concentration Measurements, Pipeline Research Council International (PRCI) 2021 Virtual Research Exchange, March 4, 2021. (**Invited Presentation**).

## 9.5 METEC Research Alerts

1. Jayarathne, J. R. R. N., R. S.KolodziejIV, S. N. Riddick, D. J.Zimmerle, and K. M. Smits. 2022. For Leaks in Snow and Ice Conditions, Experiments Show Faster Gas Migration, Higher Gas Concentrations, and Continued Gas Migrations Days after Leak Was Stopped.**METEC Research Alert**, April 5, 2022.
2. Jayarathne, J. R. R. N., R. S.KolodziejIV, S. N. Riddick, D. J.Zimmerle, and K. M. Smits. 2022.For Leaks in Rain, Snow, and Ice Conditions, Experiments Show Faster Gas Migration, Higher Gas Concentrations, and Continued Gas Migrations Days after Leak Was Stopped.**METEC Research Alert**, Sept 9, 2022.

## 9.6 Media Reports

1. Marcellus Drilling News (2022, Oct 7). Soil Moisture plays key role in spread of methane from pipe leaks. MarcellusDrilling.com <https://marcellusdrilling.com/2022/10/soil-moisture-plays-key-role-in-spread-of-methane-from-pipe-leaks/>
2. Knoxville News Sentinel, Nashville leans toward natural gas in quest to stop burning coal, <https://www.knoxnews.com/restricted/?return=https%3A%2F%2Fwww.knoxnews.com%2Fstory%2Fnews%2Fenvironment%2F2022%2F11%2F03%2Ftva-nashville-tn-leans-toward-natural-gas-in-quest-stop-burning-coal%2F69610589007%2F>, by Anila Yoganathan, Nov 4, 2022.
3. Southern Methodist University Newsroom, “Study reveals soil moisture plays the biggest role in underground spread of natural gas leaking from pipelines.” Available at: [Study reveals soil moisture plays the biggest role in underground spread of natural](#)

- gas leaking from pipelines - SMU, October 25, 2022, Study highlighted in [Science Daily](#), [Physics Org](#), and [Marcellus Drilling](#)
4. Navodi Jayarathne. Back To the Field on AGU Tumbler July 26, 2021. <https://americangeophysicalunion.tumblr.com/post/657785075107332096/back-to-the-field-hello-from-the-methane>
  5. Smits' Research Group Performs Experiments Alongside U.S. Air Force Academy. SMU Lyle Internal News. <https://blog.smu.edu/lyle/2023/09/28/smits-research-group-performs-experiments-alongside-u-s-air-force-academy/>

## 10. **References**

- Blankinship, D., Grise, S., & Schottke, J. (2008). *Fire Service/HazMat GIS Data Model Implementation Guide Prepared in cooperation with the National Association of State Fire Marshals* (Issue March).
- Cho, Y., Ulrich, B. A., Zimmerle, D. J., & Smits, K. M. (2020). Estimating natural gas emissions from underground pipelines using surface concentration measurements. *Environmental Pollution*, 267. <https://doi.org/10.1016/j.envpol.2020.115514>
- Gao, B., Farnsworth, J., & Smits, K. M. (2020). Evaporation from undulating soil surfaces under turbulent airflow through numerical and experimental approaches. *Vadose Zone Journal*, 19(1). <https://doi.org/10.1002/vzj2.20038>
- Gao, B., Mition, M. K., Bell, C., Zimmerle, D., Deepagoda, T. K. K. C., Hecobian, A., & Smits, K. M. (2021). Study of methane migration in the shallow subsurface from a gas pipe leak. *Elementa: Science of the Anthropocene*, 9(1). <https://doi.org/10.1525/elementa.2021.00008>
- Hildebrand, M. S., & Noll, G. G. (2017). *Pipeline Emergencies* (Third Edit, p. 21). NATIONAL ASSOCIATION OF STATE FIRE MARSHALS Cheyenne, WY 82003.
- Jayarathne, J. R. R. N., Kolodziej, R. S., Riddick, S. N., Zimmerle, D. J., & Smits, K. M. (2023). Influence of soil-gas diffusivity on expansion of leaked underground natural gas plumes and application on simulation efforts. *Journal of Hydrology*, 625(PB), 130049. <https://doi.org/10.1016/j.jhydrol.2023.130049>
- Mitton, M. (2018). Subsurface Methane Migration From Natural Gas Distribution. *Faculty and the Board of Trustees of the Colorado School of Mines*. <https://mountainscholar.org/handle/11124/172530>

- National Volunteer Fire Council, United States Department of Transportation, & Pipeline and Hazardous Materials Safety Administration. (n.d.). *Fire Department Pipeline Response, Emergency Planning, and Preparedness*.
- NTSB. (1979). *NTSB PAR 79-3 Pipeline Accident Report*.
- Patterson, B. M., & Davis, G. B. (2009). Quantification of vapor intrusion pathways into a slab-on-ground building under varying environmental conditions. *Environmental Science and Technology*, 43(3), 650–656. <https://doi.org/10.1021/es801334x>
- PHMSA. (2024). *Gas Distribution Incident Data - January 2010 to Present*. <https://www.phmsa.dot.gov/data-and-statistics/pipeline/distribution-transmission-gathering-liquid-and-liquid-accident-and-incident-data>
- Pipeline Emergency Response Guidelines* (2018 Edition, pp. 1–17). (2006). Pipeline Association for Public Awareness.
- Poulsen Tjalfe G., G., Christophersen, M., Moldrup, P., & Kjeldsen, P. (2003). Relating landfill gas emissions to atmospheric pressure using numerical modelling and state-space analysis. *Waste Management and Research*, 21(4), 356–366. <https://doi.org/10.1177/0734242x0302100408>
- Riddick, S. N., Bell, C. S., Duggan, A., Vaughn, T. L., Smits, K. M., Cho, Y., Bennett, K. E., & Zimmerle, D. J. (2021). Modeling temporal variability in the surface expression above a methane leak: The ESCAPE model. *Journal of Natural Gas Science and Engineering*, 96. <https://doi.org/10.1016/j.jngse.2021.104275>
- Ulrich, B. A., Mitton, M., Lachenmeyer, E., Hecobian, A., Zimmerle, D., & Smits, K. M. (2019). Natural gas emissions from underground pipelines and implications for leak detection. *Environmental Science and Technology Letters*, 6(7), 401–406. <https://doi.org/10.1021/acs.estlett.9b00291>
- Vetter, C. P., Kuebel, L. A., Natarajan, D., & Mentzer, R. A. (2019). Review of failure trends in the US natural gas pipeline industry: An in-depth analysis of transmission and distribution system incidents. *Journal of Loss Prevention in the Process Industries*, 60(January), 317–333. <https://doi.org/10.1016/j.jlp.2019.04.014>
- Zimmerle, D. J., Pickering, C. K., Bell, C. S., Heath, G. A., Nummedal, D., Pétron, G., & Vaughn, T. L. (2017). Gathering pipeline methane emissions in Fayetteville shale pipelines and scoping guidelines for future pipeline measurement campaigns. *Elementa*, 5, 1–12. <https://doi.org/10.1525/elementa.258>





## **11. Appendix**

Appendix 1: Survey of first responder operational practices: First responder operational practices when attended large pipeline leak events

Appendix 2: Performance Testing of SGX Integrated Infrared (INIR) sensor in subsurface methane detection

Appendix 3: RPLUME / UPSIDE Data Management Protocol

Appendix 4: Report on a Practical Approach to the Design, Operation, and Monitoring of Soil Aeration

Appendix 5: Understanding of the degree to which parameters affect the subsurface natural gas migration with significant flow rates: Experimental Report

Appendix 6: Understanding of the degree to which parameters affect the subsurface natural gas migration with significant flow rates: Simulation Report

Appendix 7: Underground Natural Gas Pipeline Leak Behavior: Connecting gas migration understanding to first responder protocols

